NASA CONTRACTOR REPORT

INVESTIGATION OF THREE CLASSES OF COMPOSITE MATERIALS FOR SPACE VEHICLE APPLICATION

by John A. Alexander, J. C. Withers, and B. A. Macklin

Prepared by
GENERAL TECHNOLOGIES CORPORATION
Alexandria, Va.

NATIONAL AERONAUTICS AND SPACE ADMINISTRATION • WASHINGTON, D. C. • MAY 1967

NASA CR-785

INVESTIGATION OF THREE CLASSES OF COMPOSITE MATERIALS FOR SPACE VEHICLE APPLICATION

By John A. Alexander, J. C. Withers, and B. A. Macklin

Prepared under Contract No. NASw 1347 by
GENERAL TECHNOLOGIES CORPORATION
Alexandria, Va.

for

NATIONAL AERONAUTICS AND SPACE ADMINISTRATION

For sale by the Clearinghouse for Federal Scientific and Technical Information
Springfield, Virginia 22151 – CFSTI price $3.00

ABSTRACT

Fabrication, development and characterization was conducted on continuous filament reinforced whisker reinforced and multilaminar composites. Four techniques for continuous filament composite formation were investigated; electrodeposition with concurrent filament winding, the hot pressure bonding of electrolytically deposited monolayer tapes, the hot pressure bonding of foil filament arrays and liquid metal infiltration. The tensile, compressive and flexure properties of W-Ni, B-Al and B-Mg composites are compared. The best compressive and flexure strength results were at least double the tensile values while compressive and flexure moduli were quite low. A technique for the accomplishment of aligned whisker yarns by dry spinning textile techniques and the subsequent infiltration of aligned whisker arrays by electrodeposition yielded composite samples with strengths ranging between 226×10^3 psi and 327×10^3 psi, which calculate to whisker strength utilization in excess of one million psi. The feasibility of high volume production of infiltrated aligned whisker wires by a combination of textiling and continuous electroplating technology is clearly demonstrated. Deposition techniques for the formation of multilaminar Mo-TiB_2 composites have been developed which yield good interphase bonding.

TABLE OF CONTENTS

LIST OF ILLUSTRATIONS

LIST OF ILLUSTRATIONS

LIST OF ILLUSTRATIONS

LIST OF ILLUSTRATIONS

LIST OF ILLUSTRATIONS

LIST OF TABLES

INTRODUCTION AND SUMMARY

The research program described in this report was intended to be an investigation of the properties of three types of composite materials for the purpose of developing these materials for space vehicle structural applications. Filament reinforced metal matrix composites, whisker reinforced metal matrix composites and laminar metal-ceramic composites were included in this investigation. The experimental program involved the development of fabrication procedures for the generation of samples of each type of composite and the determination of various mechanical properties of the generated samples.

The interest in composite materials is based on the insufficiencies of conventional materials in the satisfaction of design requirements for advanced space vehicle applications. The con cept that two or more materials can be combined in such a fashion as to perform more efficiently than either material alone is the basis for the development of composite materials. It should be emphasized that this concept requires that a significant jump in available materials properties be the objective of composites development programs, for the promise of composite materials is based on their ability to provide new and better materials rather than to simply replace the old.

Three types of composites, filament, whisker and multilaminar, have received much attention in the multitude of review articles written in recent years on the potential of such materials. Theoretical calculations of the material properties predicted for composites have expanded the size of the expectations for these materials. However, experimental verifications of the high expectations were quite limited when this program was initiated. The effort undertaken at the General Technologies Corporation (GTC) was intended to provide experimental verification of the potential of these three types of composite materials and to provide a basis for concentrated development effort in each. The three areas of work are treated separately in this report because the fabrication processes, the experimental techniques and the degrees relative progress have been quite different.

The multilaminar composites work utilizing the system Mo-TiB_2 has resulted in the development of vapor deposition techniques for their formation. The problems involved in achieving an interlaminal bond sufficient to test the proposed behavior of such materials are described. The filament reinforced composite materials work involved the continued development of the electroforming technique for composite fabrication utilizing the system Ni-W and Al-B. Electrodeposition techniques for monolayer tape formation in the Al-B system are discussed along with hot pressure bonding techniques for forming monolayer tapes into multilayer composites. Composites of the Mg-B system were fabricated by

hot pressure bonding of foil-filament arrays and by liquid metal infiltration. While most composite development programs have been limited to determination of tensile strength and modulus values for experimental composite materials, this program was directed toward the generation of strength and modulus data in compression and flexure as compared to base line tensile values from the same types of composites. Finally, the effort on whisker composites was concentrated on the means for the accomplishment of aligned whisker composites. The program focused on the experimental evaluation of various proposed alignment schemes and ultimately resulted in the development of a textile type spinning operation for long whisker fibers and infiltration by electrolytic deposition techniques. The well infiltrated whisker composites demonstrated that whisker strength utilization in excess of one million pounds per square inch can be accomplished. Of particular import in this work is the susceptibility of the developed process to mass production via textile technology and continuous electro or vapor deposition techniques. Specific areas for future concentrated effort are singled out based on the experimental effort conducted under this program and the developments in the composites field in general during the past year.

WHISKER REINFORCED COMPOSITES

The discovery that the whisker form of many crystalline materials exhibit extraordinarily high strengths has excited much basic research into the origin of such strength.[1, 2, 3, 4, 5]. The technologies for growing whiskers of a wide variety of materials have been developed and gram to pound quantities of SiC and Al_2O_3 are grown and sold commercially. Because of their exceedingly small size the practical utilization of whisker strength will involve their successful incorporation in matrices capable of transferring load to the whisker. Numerous review articles have been generated over the past few years which accentuate the "potential" of whisker reinforced composite materials [6,7,8,9,10,11,12,13,14, 15,16,17,18,19]. At the time of his review Cratchley [10] indicated that while there had been great speculation as to the properties which might be expected from whisker composites, this field of reinforcement was the farthest away from providing practical composite materials. His summarization of the problems of whisker compositing served as the basis for the work initiated under this portion of the program. "As the strongest whiskers seem to be the small ones, the problems of growing, harvesting, aligning and incorporating them are greatly magnified. However, the potential advantages of whisker reinforcement for high strength/weight ratios at elevated temperatures appear to be greater than those offered by the majority of other fiber-reinforced systems and it may be that the extra effort will eventually prove worthwhile".

The extent of success at the time of initiation of this effort can be summarized in the work of Sutton and co-workers[6,16,20,21,22] with alumina in silver and by Parratt [23] with silicon nitride in silver. Both investigators demonstrated significant room and elevated temperature strength enhancement. Kelsey[24] reported a 280% improvement in the tensile strength of a 36 v/o alumina reinforced iron powder-fabricated specimen.

With this limited experimental background for the heavily documented potential of whisker composite, the General Technologies Corporation undertook to demonstrate whisker reinforcement of metal matrix composites utilizing room temperature electrodeposition techniques for matrix infiltration and concentrating on techniques of whisker alignment which would lend themselves to continuous production processes.

Since the initiation of effort on this program relatively little new experimental data have been generated [25,26,27,28,29,30,31]. However, concurrent with the preparation of the Final Report on the first years effort at GTC in the area, Dr. Richard H. Krock summarizes the state of the art with the following words.

"The mechanics of coupling disparate materials together are tricky, but well established by now. Unhappily, though, practical whisker composites still elude us, despite a plethora of laboratory specimens. The reason is that such composites

are proving exceedingly difficult to make. No satisfactory way has yet been found for getting thousands of delicate whiskers packed into the matrix, properly aligned, bonded, and with their strengths unimpaired so as to be able to accept loads from the matrix."

It is the objective of the report of the work conducted on this program at the General Technologies Corporation to show that a satisfactory way has been found to incorporate these whisker materials into a matrix, properly aligned, bonded and with their strengths unimpaired as indicated by the high strengths achieved with specimen fabricated by a process susceptible to continuous scale-up.

It was the preconcieved notion of the effort at the General Technologies Corporation that whisker alignment was essential to the accomplishment of high volume percent loadings and optimized utilization of whisker strength. A survey of the surveys indicated that the following alignment techniques had been proposed for the preparation of aligned whisker metal matrix composites:

1. Extrusion
2. Rolling
3. Centrifugal Casting
4. Magnetic Field Techniques
5. Electrostatic Charge Techniques
6. Hand Arrangement and Liquid Metal Infiltration

The organization of the program involved the evaluation of the potential of these processes by survey efforts with each technique. The first result of actual exposure to the attempted manipulation of whiskers and whisker arrays in various kinds of powder or fluid media is the appreciation of the extreme contrariness of their behavior. Randomly oriented whiskers can be likened to arrays of broom sticks. An array with random orientation occupies a very small volume percent of the space it fills. For example, the bulk density of Thermokinetic Fibers, Inc. 3B sapphire whiskers when randomly settled in air is about 0.6 g/cc, which is equivalent to a volume content of 18% whiskers. Any randomly oriented 3B whisker array will be limited to approximately that volume percent of whiskers. To attain any higher volume percent loading the whiskers must be broken and packed by brute force or they must be aligned. Brute force packing suffers from the continually decreasing ℓ/d ratio of the packed whiskers as the volume percent loading is increased. Even at much lower volume percent loadings (5 to 10%), whiskers tend to cluster together and create log jammed arrays.

The survey of alignment procedures at GTC was initiated with whisker loadings in the 5 to 10 v/o range and work was conducted on extrusion, centrifugal casting, rolling and magnetic alignment. The extrusion and centrifugal casting were initially conducted using transparent resins as matrices. A simple square-faced extrusion cylinder with a 16/1 and a 20/1 extrusion ratio yielded whisker reinforced matrices which showed

relatively good surface alignment but substantial misalignment in the center of the resulting rod. Recent effort by Wohrer[30] and Shaver[33] have indicated that a good degree of whisker alignment is attainable by extrusion if care is taken to avoid turbulent flow by step reductions with much lower extrusion ratios.

Centrifugal casting experiments involved the curing of whisker resin mixtures in a glass tube rotating at 500 to 3500 r.p.m. and by techniques involving repeated stop-start rotational cycles. The fluid shear involved in the initial start-up of the rotating tube seemed more effective than rotational speed since the start-stop samples showed maximum alignment. The surface alignment in such specimens can be observed in Figure 1. Experiments with centrifugal casting were shifted to a metal matrix on the basis of the resin survey experiments and a casting chamber of the form shown in Figure 2 was constructed first with a steel chamber and later with a graphite chamber.

Whiskers in the amount of 5 to 10 v/o were added to aluminum powder and codispersed in alcohol to accomplish cluster break up and homogenous distribution of whiskers. The mass was dried and utilized as a charge for the casting chamber. Specimens were prepared by bringing the chamber to a temperature of 710°C, 800°C and 900°C and then initiating the rotation of the chamber; by putting the chamber in motion while the powder-whisker mixture was being brought to temperature; and by utilizing a start-stop technique after bringing the chamber to liquefaction temperature. Segregation of the whiskers to the oxide skin layer was observed and minimization of the oxide layer by the utilization of protective fluxes and inert atmosphere was unsuccessful. In general the whiskers were highly segregated with little indication of the accomplishment of alignment. Figure 3 is a cross section of centrifugally cast specimens containing roughly 1% whiskers from a powder whisker mix of 5%.

The attempts at the accomplishment of whisker alignment by hot rolling were conducted on sapphire whisker mats which were nickel carbonyl coated to make them conductive and electrolytically infiltrated with nickel. An apparatus for vapor plating of nickel via the nickel carbonyl reaction: $Ni(CO)_4 \xrightarrow[70-125°C]{\text{catalyst}} Ni + 4\,CO$ had been constructed.

The schematic of that system is shown in Figure 4 and pictured in Figures 5 and 6. The reaction chamber consists of a glass chamber with an axially positioned central glass tube that is internally resistance heated. An as-grown whisker mat is attached to the axial glass tube, heated to 80°C by the internal resistance wire and the carbonyl and catalyst are added with an argon carrier gas. Care is taken to assure that the whisker mat is in intimate contact with heated glass tube; a uniformly coated whisker mat can be produced in approximately 45 minutes.

GTC 56-1

Figure 1. Al_2O_3 Whiskers Aligned by Centrifugal Casting in an Epoxy Resin

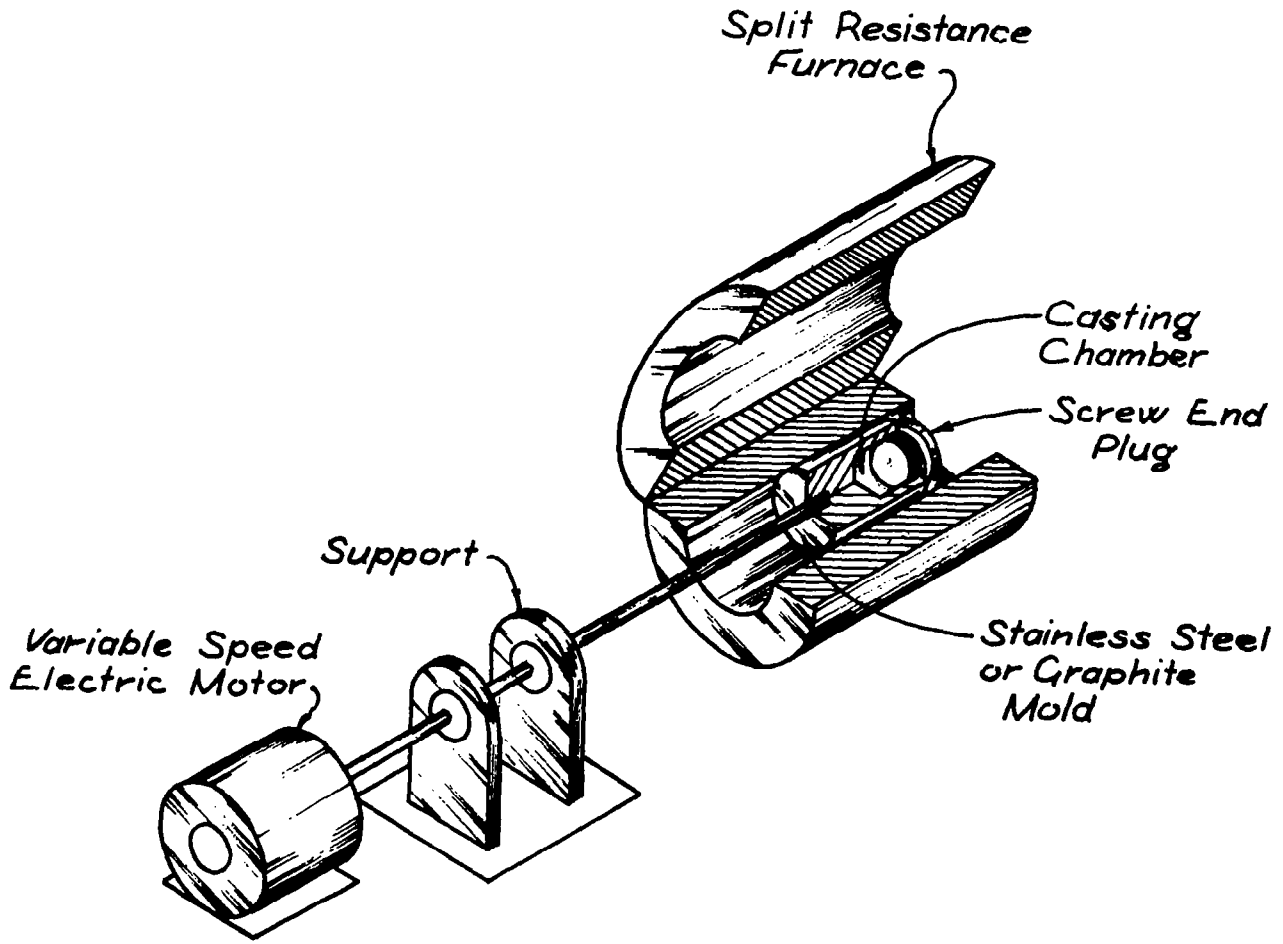

Figure 2. Aluminum Centrifugal Casting Apparatus

GTC 56-2

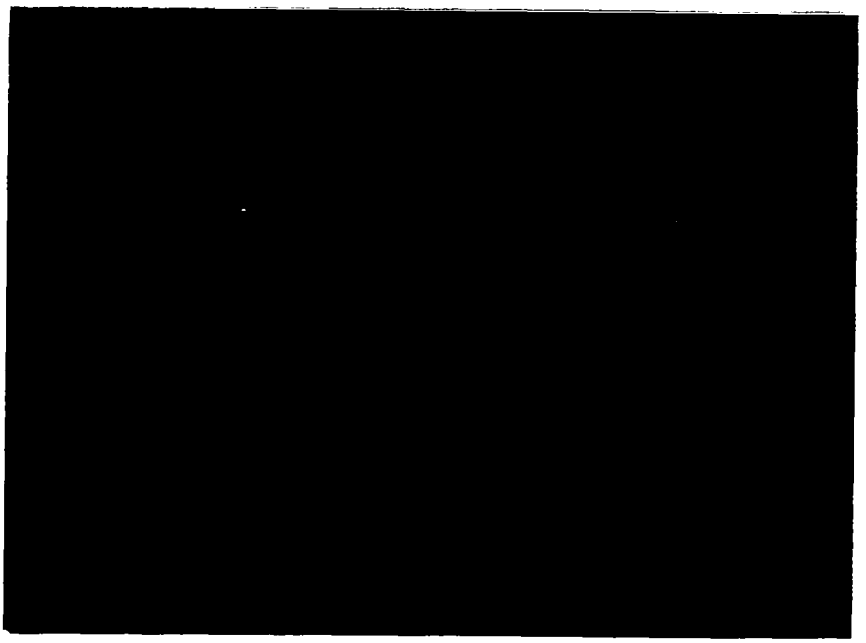

Figure 3. Cross-section of a Cast 7075 Aluminum-Low Volume Percent Sapphire Whisker Composite.

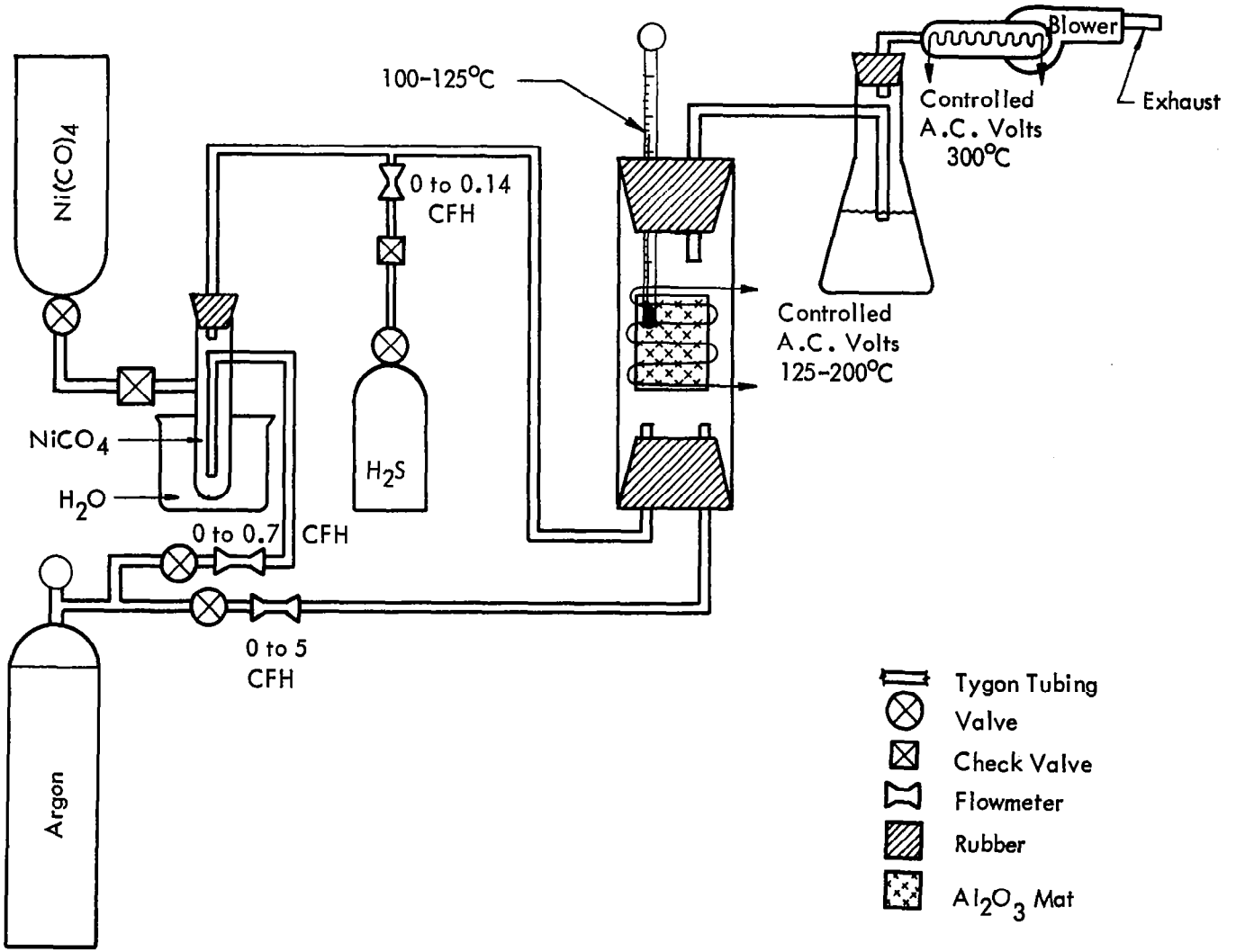

Figure 4. Apparatus for the Vapor Deposition of Ni from $Ni(CO)_4$ on to Al_2O_3 Whisker Mat.

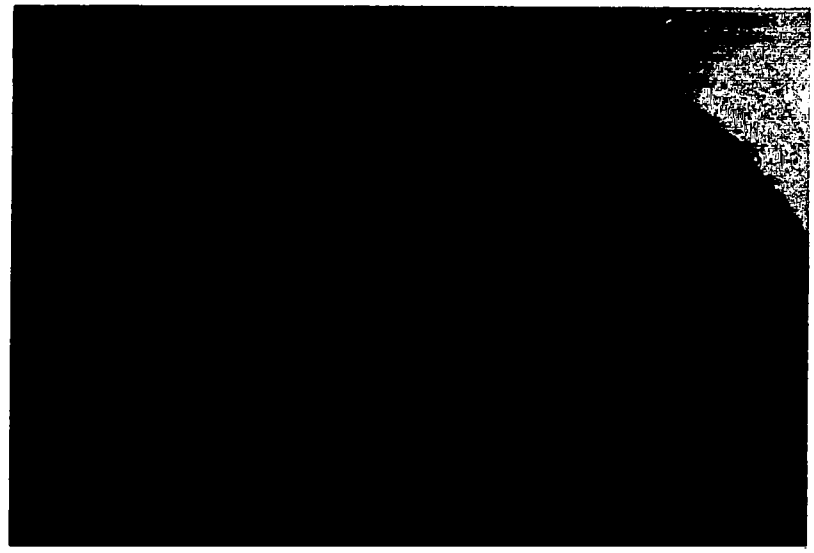

Figure 5. Overall View of Nickel Carbonyl Deposition Apparatus

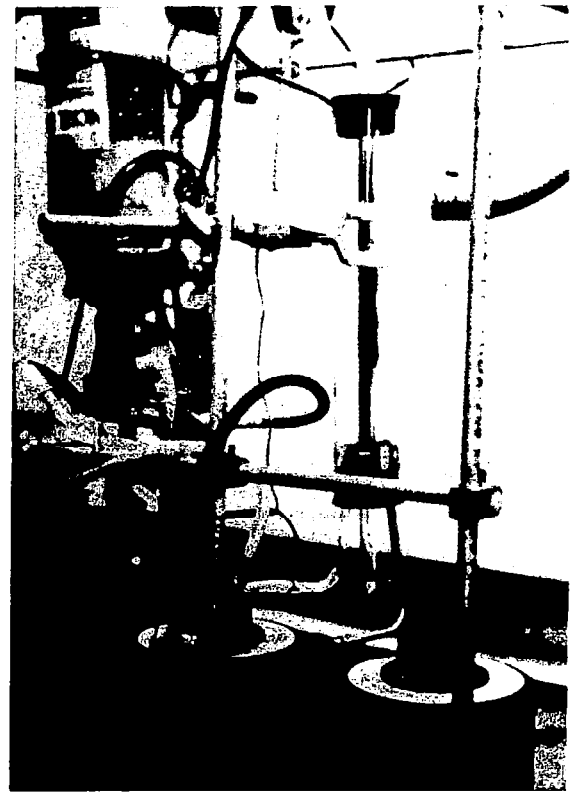

Figure 6. Nickel Carbonyl Reaction Chamber

These coated mats were removed from the apparatus and placed in commercial sulfamate plating bath and plated at a relatively low current density for 24 hours. Figures 7 and 8 show a typical cross section of as-plated whisker mats. The electrodeposition proceeds on all of the coated whiskers initially but as time passes the external whiskers plate faster than those on the interior and the resultant specimen has a high degree of internal voids.

Strips of Al_2O_3 whiskers were cut from the same as grown whisker mat coated by the nickel carbonyl process and infiltrated electrolytically at relative high and low current densities. High current density plating results in rapid closure of this external surface of the mat and yielded a high volume percent of voids as shown in Figure 7. A trickle current results in much slower infiltration but reduces the void concentrations as shown in Figure 8. Specimens containing these relatively high contents were cold rolled and hot rolled to approximately 50% reduction. It should be emphasized that these reductions were reductions in the external dimensions and reflected substantial void elimination rather than actual hot working of those degrees. An as-infiltrated and a typical rolled cross-section are shown in Figures 9 and 10. The scalloped marking in Figure 10 are the seam lines of preexisting voids which have been closed. Such rolling operations showed no signs of significant alignment and specimen digestion indicated high degrees of whisker breakup.

A more encouraging set of experiments indicated that nickel carbonyl coated whiskers could be magnetically aligned but utilization of that technique for the accomplishment of high volume percent loadings in specimens which could be informatively tested was impossible. Whisker mats were coated with thin layers of nickel in the carbonyl apparatus described above.

For alignment experiments the nickel coated whisker mat is placed in alcohol in a food blender and mixed at a low speed for 30 seconds and then at high speed for 5 minutes. The dispersed whisker solution is filtered in a vacuum Buchner filter and then picked up magnetically. Nickel coated sapphire whiskers were sprinkled onto a bar magnet in order to assess their behavior in a magnetic field. Much as iron fillings delineate the lines of force on a magnet, coated whiskers align in the direction of the lines of force. Whiskers tended to cluster at the corners of a bar magnet as shown in Figure 11 but on the face of the poles alignment as photographed in Figure 12 was observed.

As a result of the observed alignment a device for the incorporation of aligned whiskers in an electrodeposited nickel matrix was constructed. Figure 13 is the schematic of that device and shows that the circular rod magnet is inserted as a cathode in the bottom of a funnel-shaped tube with a close tolerance fit to the glass tube. The anode is placed in the top of the device and electrolyte is pumped continuously through the deposition cell. Nickel coated whiskers are added to the electrolyte at a controlled rate and are picked up in an aligned position on the magnet while electrodeposition of the nickel matrix is concurrently being

GTC 56-3

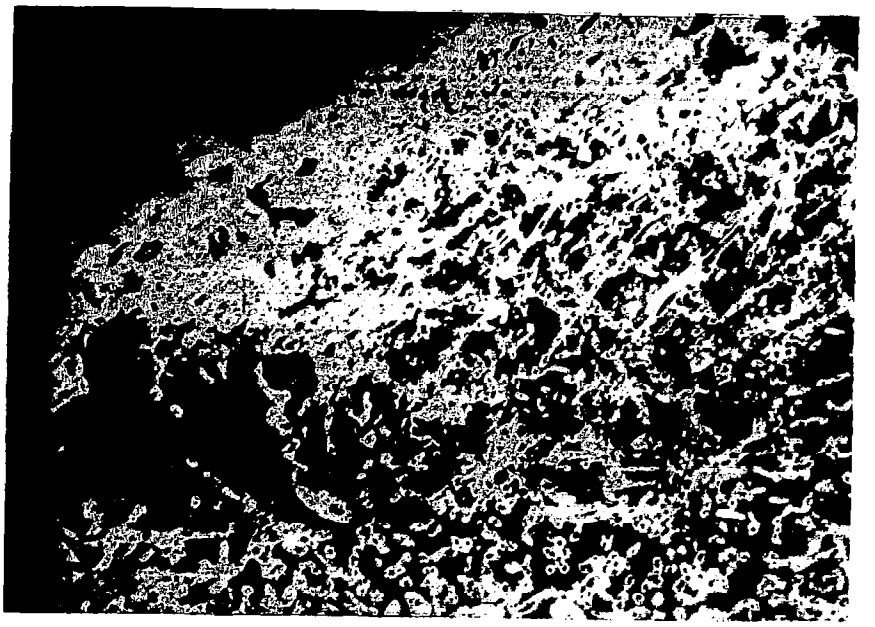

Figure 7. Electrolytic Infiltration of Carbonyl Coated Al_2O_3 Whisker Mat at a Relatively High Current Density

GTC 56-4

Figure 8. Electrolytic Infiltration of Carbonyl Coated Al_2O_3 Whiskers at a Low Current Density

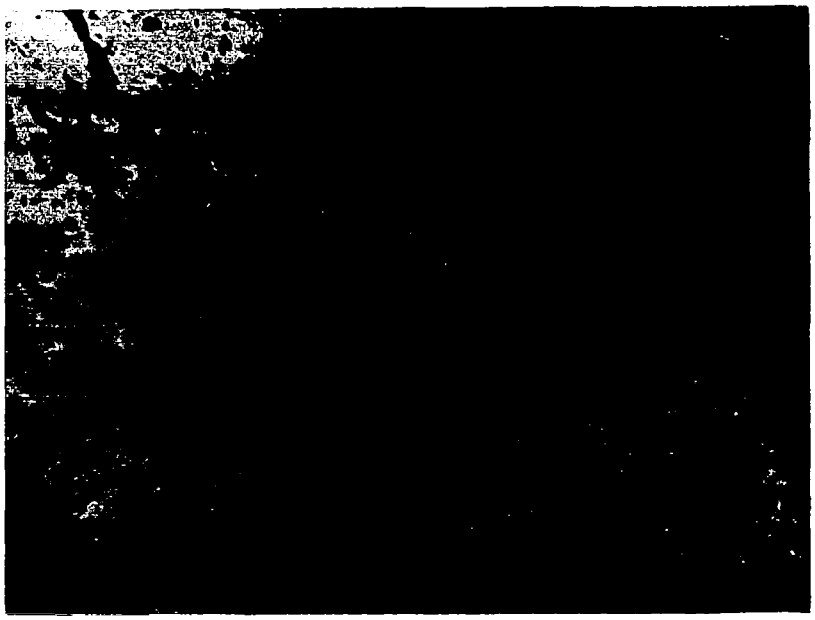

Figure 9. Cross-section of an Electrolytically Infiltrated Sapphire Whisker Mat 100X

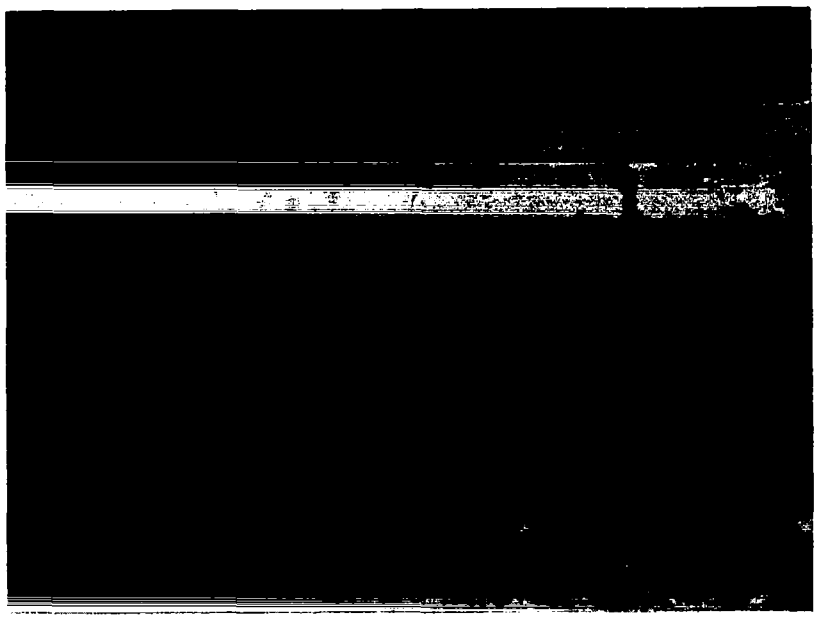

Figure 10. Cross-section of a Cold Rolled Electrolytically Infiltrated Sapphire Whisker Mat 400X

GTC 56-5

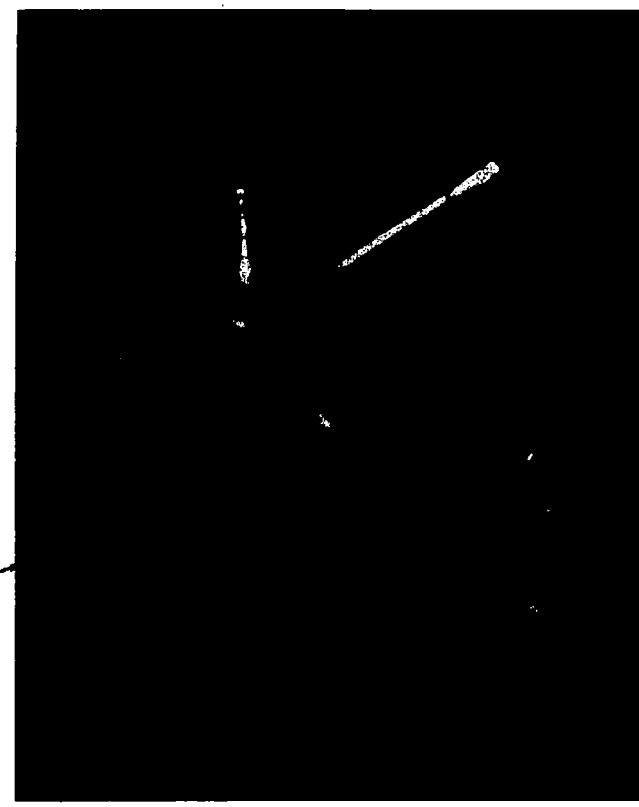

Figure 11. Nickel Carbonyl Coated Whiskers at the Corner of a Bar Magnet

GTC 56-6

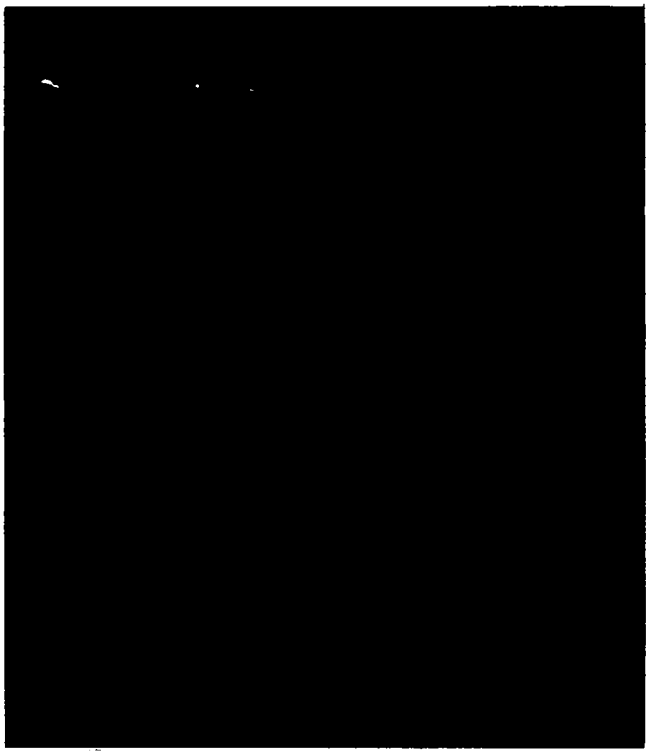

Figure 12. Nickel Coated Whiskers Aligned on a Magnet 200X

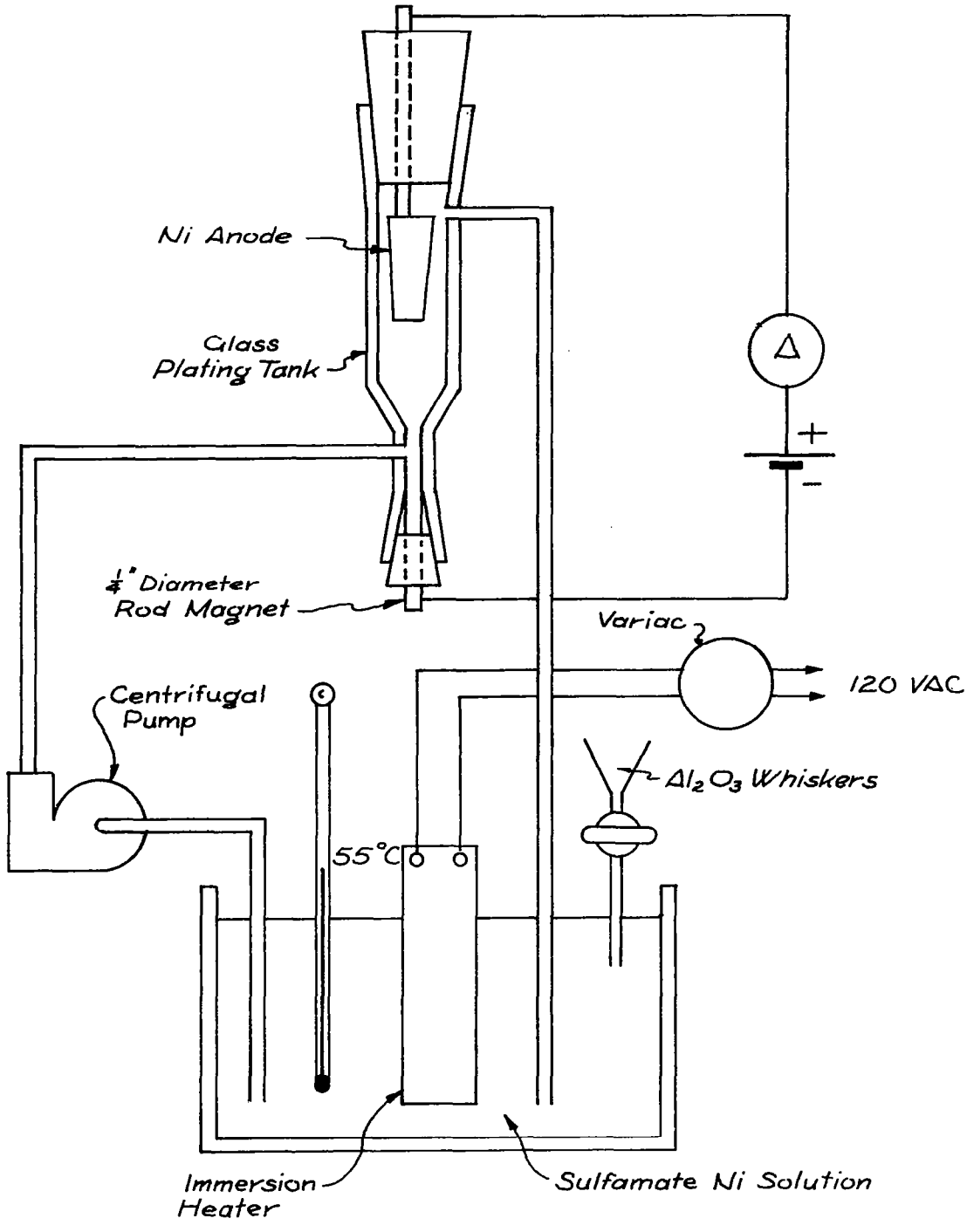

Figure 13. Apparatus for the Preferred Orientation Entrapment of Ni-Coated Al_2O_3 Whiskers in an Electrodeposited Ni Rod.

accomplished. The magnet is intended to trap circulated whiskers in an aligned orientation in a concentration dependent upon the rate of addition of the whiskers to the solution and the current density applied to the plating cell. The actual apparatus is pictured in Figure 14, and a typical cathode morphology is represented in Figure 15. Changes in current density, whisker concentration, or plate-deplate cycling had little influence on the strongly dendritic nature of the deposit. Electrostatic flocking experiments were not attempted at GTC due to the report of Kane and Lindsay [34] which reported a lack of success with such techniques as applied to discontinuous glass and titania fibers.

As the initial survey work on whisker alignment techniques was in progress, a development in the technology of growing whiskers at Thermokinetic Fibers, Inc. resulted in the generation of the capability for the production of extra long type 5A beta SiC whiskers. These whiskers ranged from 1/4 to 1 inch in length with principle cross sectional dimensions in the 5 to 10 micron range. Experimentation with this whisker wool resulted in the accomplishment of dry spinning directly from the as-grown mat to a whisker thread or yarn. Figure 16 is a photograph of these five to ten micron diameter SiC fibers.

Figure 17a is a picture of a hand-spun whisker yarn that was drawn out of a ball of as-grown, type 5A, silicon carbide whisker wool. Figure 17B and C are magnified views of the end of the whisker yarns under light and dark field illumination. It can be seen that the l/d ratio for the whiskers is long enough to permit rather tight yarn formation and the degree of alignment is excellent. A few shorter length whiskers are observed protruding at an angle from the axial direction of the yarn but alignment approaches being uniaxial. Figure 18 shows a higher magnification view of typical hand spun whisker yarn. Such whisker alignment permits volume percent loadings which approach the theoretical limit for the filling of space by rods, 90.6%, while permitting the maximum possible utilization of the strength of composited whiskers in a uniaxial direction. High volume percent loadings are desirable to maximize the strength and modulus of the composite and therefore efforts to attain aligned whisker arrays offer the most direct approach to the attainment of optimized composite properties.

The simplicity of the process and its direct susceptibility to the application of textiling technology for the generation of continuous lengths of highly oriented whisker yarn directly from the as-grown whisker wool mats provides a strong incentive to the development of infiltration techniques for metallic matrices. The as-spun whisker threads were observed to be conductive and were thus able to be infiltrated by electrodeposition techniques.

The first attempts at infiltration by electrodeposition were conducted by supporting the whisker yarn vertically in a deposition bath on a metal C-frame. A horizontal support and a technique of mounting the whisker yarn on a stainless steel backing plate were also tried. These techniques suffered from a series of deficiencies:

GTC 56-7

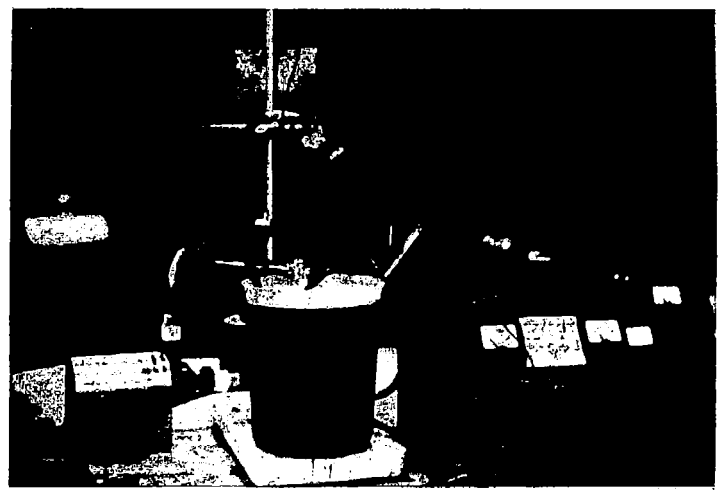

Figure 14. Magnetic Alignment Nickel Matrix Infiltration Apparatus

GTC 56-8

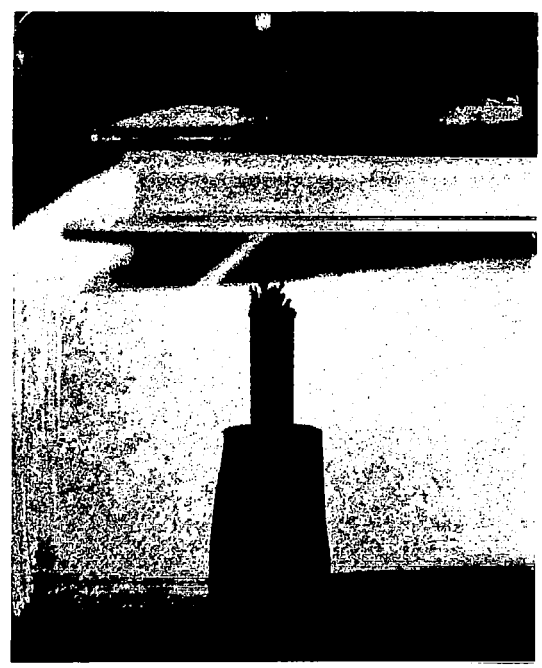

Figure 15. The Growth Configuration on the Cathode in the Magnetic Alignment Infiltration Apparatus

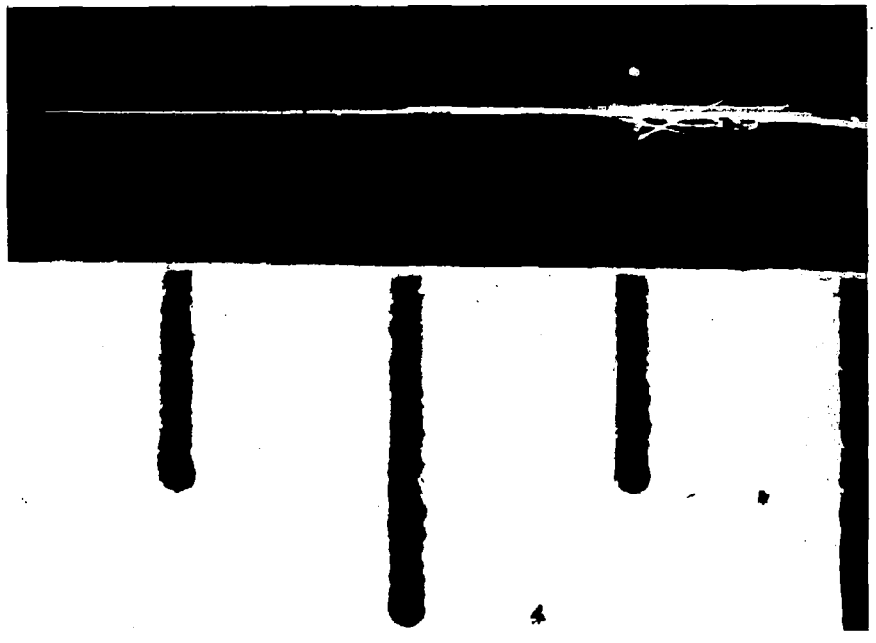

Figure 16. Five to Ten Micron Diameter SiC Fibers Shown on a 1/4 Inch Scale. The Actual Fiber Length is About 2 Inches

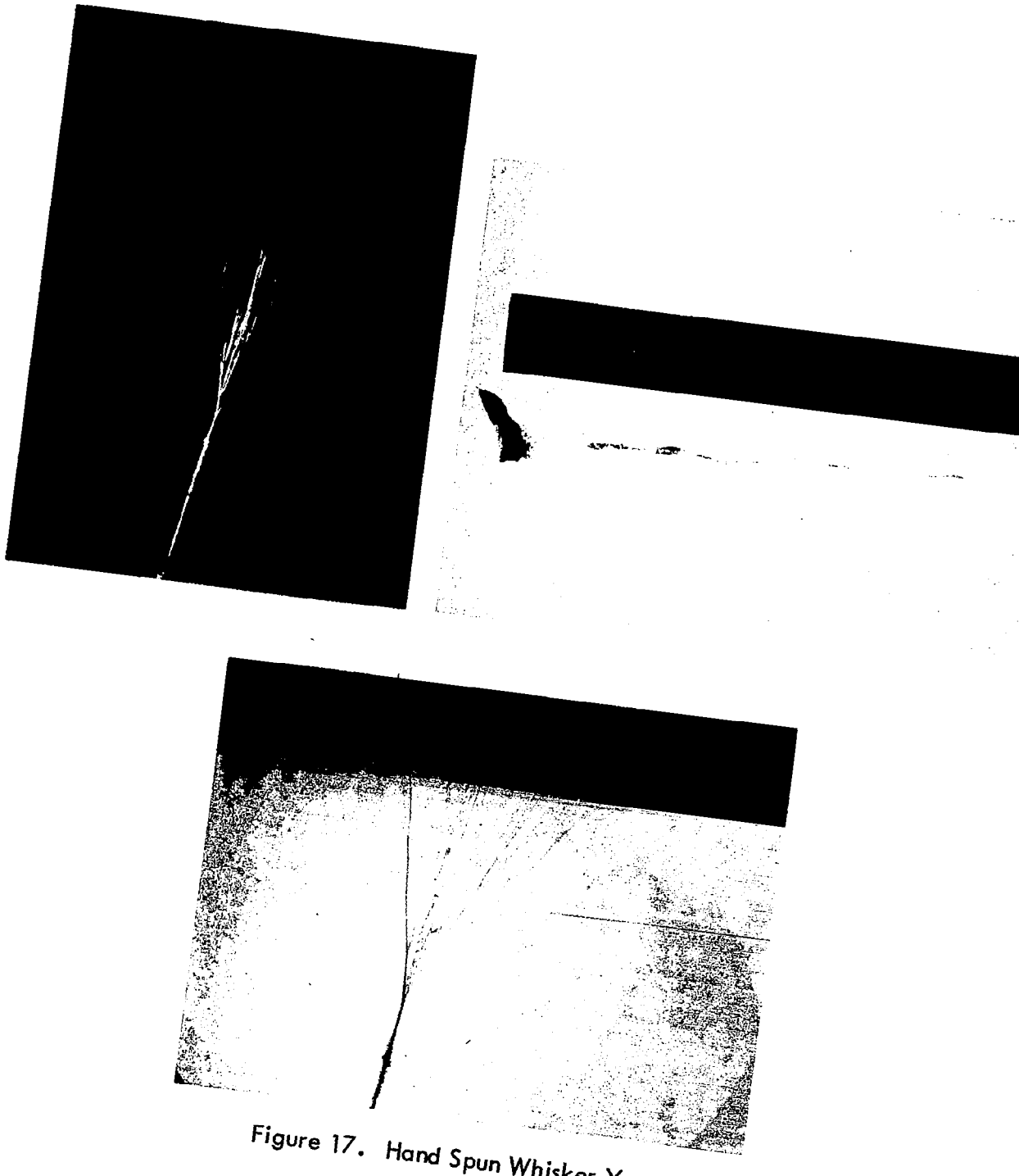

Figure 17. Hand Spun Whisker Yarns

Figure 18. Magnified View of Whisker Alignment in Hand Spun Whisker Yarn 100X

1. The conductivity of the whisker yarn was dependent upon its thickness and the tightness of spinning.

2. The infiltration generally started at the whisker yarn ends and plated toward its center.

3. The plating rate was slow.

A technique of gradual immersion was more effective. The yarn was slowly dropped into the plating bath. The tip plated first and acted as a weight to straighten the yarn as it was immersed and coated. However, this technique was relatively slow and yielded a tapered coating.

The best technique for electrolytic infiltration involved the spinning of a half mil nickel wire into the whisker yarn. A light weight could be connected to the nickel wire and electrical contact made to the other end. The ends of the spun whisker yarn were fixed to the wire with non-conductive lacquer and the balance of the wire was likewise coated to prevent plating except through the whisker yarn. Experimentation was conducted on the effect of coating rate on the fill accomplished in the whisker yarn both with and without the co-spun nickel substrate. While good fill can be accomplished with either type of yarn specimen, more consistent results are attainable with the yarns including the nickel wire. Variations in the conductivity of the yarn and the thickness and tightness of spinning were far more critical in the specimens without the nickel wire. Good quality nickel-infiltrated whisker yarns can be produced by proper control of the plating current as shown in Figure 19. The specimens prepared in this fashion were uniform on a gross scale but did have undulated surfaces. The wire specimens were further smoothed with emery paper prior to mechanical testing.

Figure 20 is a cross section of a nickel electrodeposition infiltrated aligned whisker yarn demonstrating the degree of fill attainable with this technique. One gross void is present in the cross section but fill among the aligned whiskers is excellent as shown in Figures21 and 22 at 400X and 1500X respectively. Figures 22 and 23 at 1500X are particularly informative since they not only show this high degree of infiltration but show the extent of alignment quite vividly with the perfect bulged triangle cross sections of the transverse sample and the rod like cross sections of the almost longitudinal sample. Figures 24 and 25 show 1500X pictures of two other whisker wires to indicate that both fine and coarse 5A whiskers can be aligned by textile spinning and that electrolytic infiltration is accomplished equally well in each type of array.

The mechanical properties for aligned whisker wires prepared under this program are presented in Table I. Modulus determination could be made only on specimens with a high degree of uniformity over a length of 1 to 1 1/2 inches and thus was determined on relatively few of the generated samples.

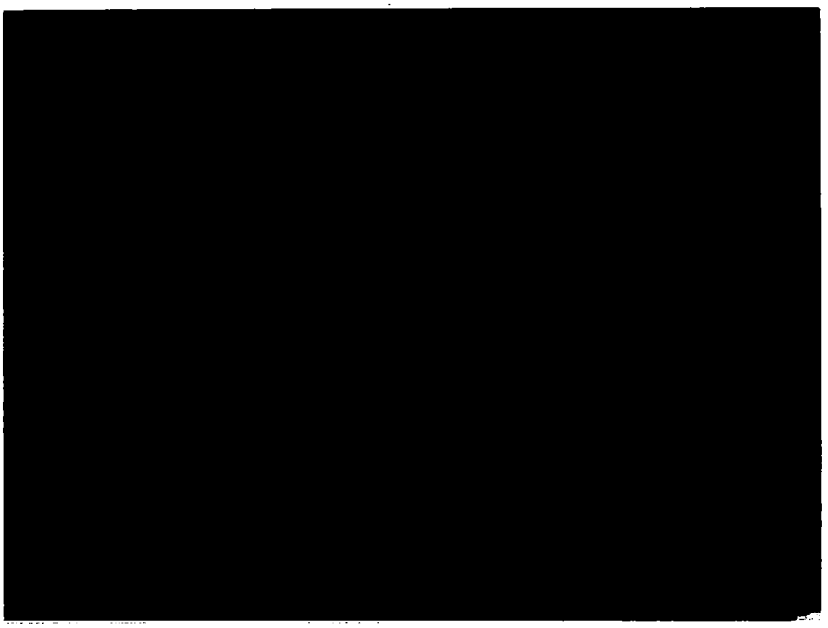

Figure 19. An Axially Aligned Whisker Yarn Infiltrated with Nickel by Electrodeposition

GTC 56-8A

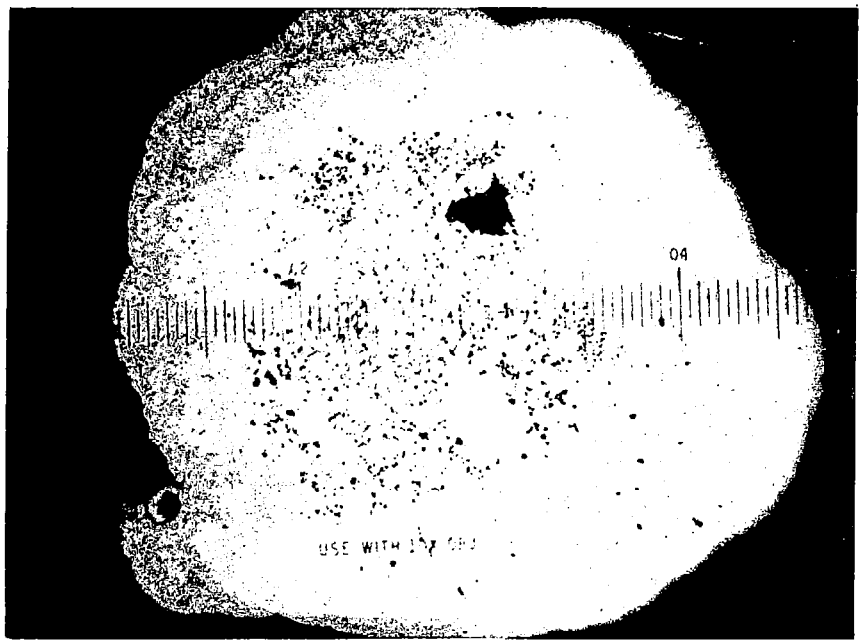

Figure 20. Cross-section of an Electrolytically Infiltrated Nickel-Silicon Carbide Whisker Yarn 100X

GTC 56-9

Figure 21. The Distribution of Whiskers in an Electrolytically Infiltrated Nickel-Silicon Carbide Whisker Composite 400X

GTC 56-10

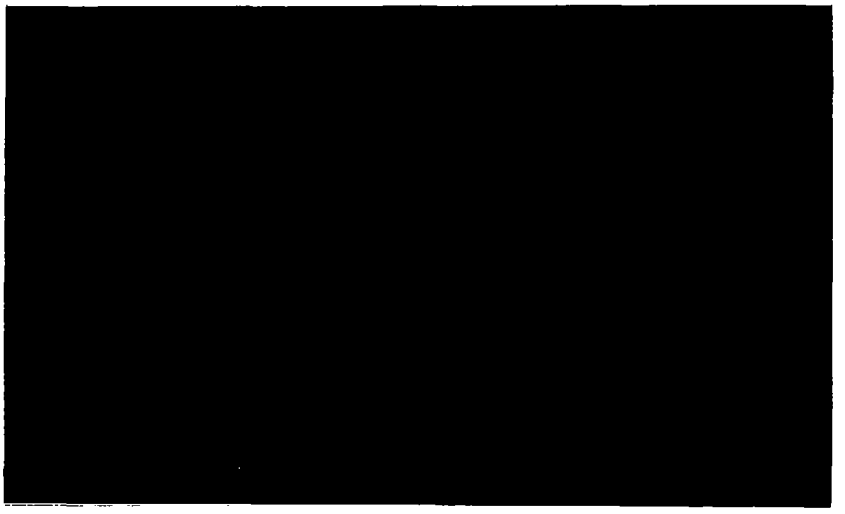

Figure 22. Transverse Cross-section of Aligned SiC Whiskers in a Nickel Matrix 1500X

GTC 56-11

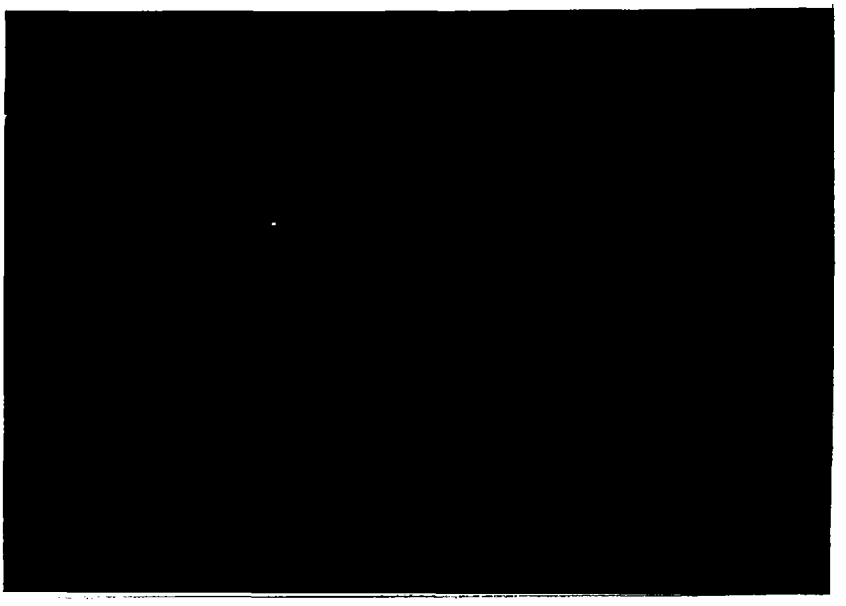

Figure 23. Longitudinal Cross-section of aligned SiC Whiskers in a Nickel Matrix 1500X

GTC 56-12

Figure 24. Nickel Infiltration of an array of Aligned Relatively Fine SiC Whiskers

GTC 56-13

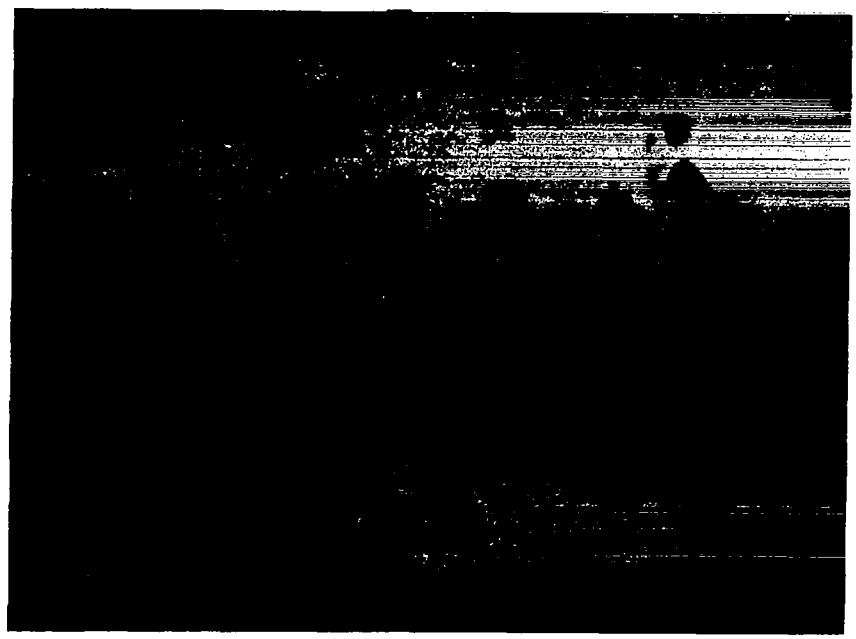

Figure 25. Nickel Infiltration of an array of Aligned Coarse SiC Whiskers

Table 1. Mechanical Properties of Nickel Infiltrated Whisker Yarn Specimens

Specimen No.	Tensile Strength (10^3 psi)	Approximate Volume Percent Whiskers	Strength Utilization of Incorporated Whiskers (10^6 psi)
II-E10	85.1		
II-E11	183	8	1.0
II-E12	92.3		
II-E13	>215	8	>1.4
II-E20	170		
II-E21	169		
II-E22	226	10	1.3
II-E23	226	10	1.3
II-E24	>185		
9 A 1	90.5		
9 A 2	>240	10	>1.4
9 A 3	327	10	2.3
10 A 1	144		
10 A 2	184		
10 A 3	234	8	1.7
33 A	53.4		
33 B	51.7		
33 C	100		
35 A	136		
35 B	188	9	1.0
45 A	163		
45 B	249	9	1.7
52 A	218	9	1.3
52 B	197		
55	64.5		
56 A	188		
56 B	288	10	1.9
66	65.8		
Electrodeposited Nickel on 1/2 mil Ni Wire			
50 A	90.5	0	
50 B	84.0	0	
60 A	105	0	

Perfect uniformity in the spun yarn is not a characteristic of the spinning process in its current state of development. The variations in whisker density along the spun yarn dictates that the infiltrated wire will fail at the cross section containing the minimum volume percent whiskers. The low strength values represent the first test on a single yarn. Subsequent retests eliminate the weak points and yield the higher values. The volume percent loading cannot be derived from inspection of the fracture cross section. The specimen must be mounted and polished back to yield a metallographic surface for evaluation. The detailed work required to accurately assess the generated data is time consuming but every effort was being made to extract the maximum amount of information from each prepared whisker reinforced specimen. The technique for generating the mechanical property data must be described in detail in order to demonstrate that the values generated are indicative of the potential of aligned whisker reinforced metal matrix composite even though the sample itself is unconventional.

The whisker yarn is spun with special care being taken to minimize the irregularities in the thickness and in the tightness of the yarn. Yarn specimens that were highly irregular were used to evaluate the infiltration potential while uniform speciment were utilized for mechanical test. The whisker wires were mounted in epoxy on pin tabs and tested on the Universal Testing machine. Specimens with a gauge length in excess of 1" were monitored with a mechanical extensometer for elongation to yield a complete stress-strain curve for the composite. After testing to failure the fracture cross section was examined microscopically and its cross-sectional area estimated. Figure 26 is a typical whisker wire fracture cross section. The shortest wire segment was mounted for metallographic preparation and a minimum of length was ground back to yield a complete cross section of the whisker wire. The wire fracture cross-sectional area was superimposed upon the area with the greatest density of aligned whiskers as shown below:

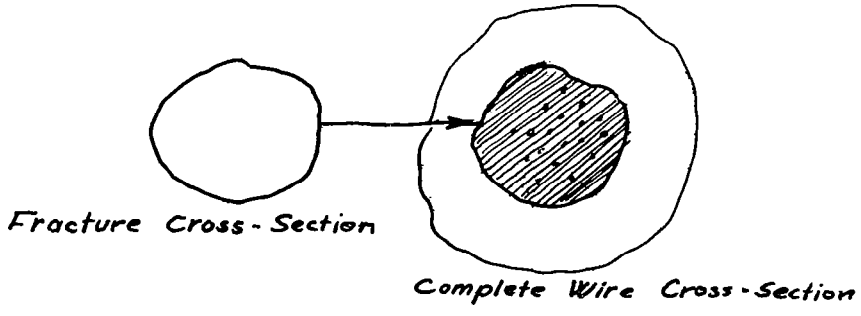

The whisker content of the fracture cross-sectional area was estimated utilizing point count lineal analysis and by cut-out of whiskers from the photomicrograph and weighing the matrix and whisker portion of the photomicrograph. The volume percent calculation is approximate but comparison with charts of areal fraction of irregular particles indicate that the calculated values are within a percent or two of the actual values. There is no evidence of necking in the specimens examined

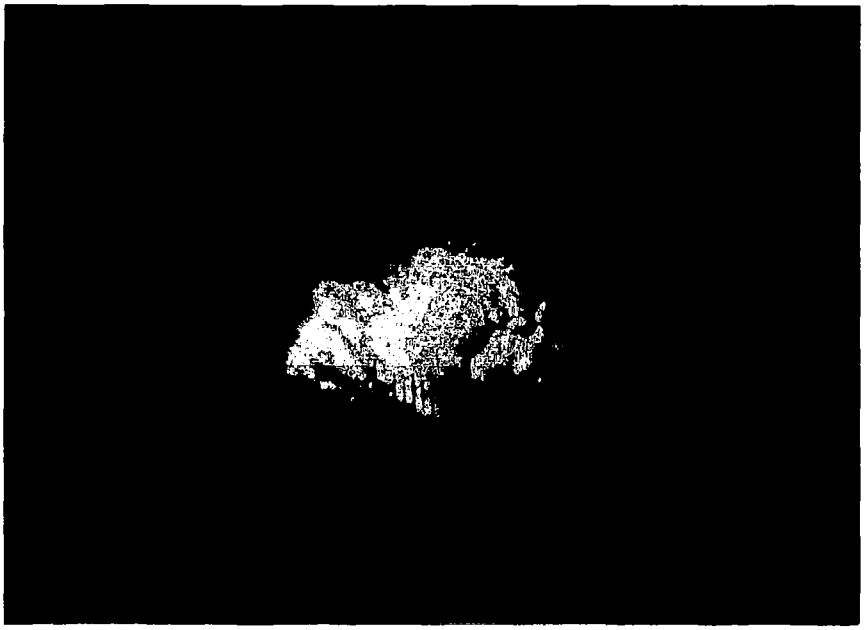

Figure 26. Typical Whisker Wire Fracture Cross-section 100X

and the assumption that all of the whiskers in the polished cross section were in the fracture cross section is conservative. No porosity is assumed in the fracture cross section and no correction has been made for such porosity even when observed in the photomicrpgraphy. Thus the generated values in Table I represent conservative approximations of the strengths which can reasonably be extracted from aligned SiC whisker reinforced nickel. Unreinforced nickel specimens were tested and the values are also included in Table I. Assuming a value of 100,000 psi for the matrix contribution, whisker strength utilization values are calculated in the final column of that table. The importance of these figures lies not in their absolute values because of the several approximations which were involved in their calculation. However, these data do reflect the pronounced effect of aligned whiskers in contributing to the strength of a metal matrix and recommend highly efforts to exploit the demonstrated strengthening capability of aligned whisker metal matrices.

Concurrent with the evaluation of hand spun-nickel infiltrated whisker yarns was the investigation of the means for mechanizing the yarn spinning process. The most encouraging development is pictured in Figure 27. The wire substrate is rotated by a variable speed motor. The whisker spinning is initiated by contact with a drop of adhesive at the head end of the wire and the whisker mat is drawn back along the wire to yield a much more uniform co-spun yarn. The spinning operation can be repeated by simple contact with the previously spun array and repetition of this process. Such a spinning operation is susceptible to scale-up for continuous operation and serves as a starting point for the conversion of as-grown whisker wool into aligned whisker arrays by processes which can be as high volume as any conventional textiling technique.

The next objective of this work was to assemble a group of nickel infiltrated aligned whisker yarns in a hot press die and form by hot pressure bonding a gross sample for mechanical test. GTC experience with SiC filament, AF 33(615)-2862, had indicated thermal stability for SiC in nickel at least 900°C for one hour. In preparation for hot pressure bonding experiments a series of pieces of composite wire were exposed to one hour heat treatments at 700°, 800°C and 900°C. The photomicrographs of the as-deposited and heat treated samples are presented in Figures 28 through 31. Obvious reactions between the single crystal whiskers and the nickel was observed after only one hour at 700°C and progressive dissolution is observed at 800°C. At 900°C essentially all whisker had been dissolved. The specificity of the dissolution process indicated that a surface layer was protecting some of the whiskers. It can be observed in Figure 30 that some triangular whiskers are imbedded on a circular sheath of dissimilar material. It is most likely that a silica or glassy layer is present on the surface of SiC whiskers and that this layer provides some protection for SiC in a nickel matrix. However, the rate of dissolution is most rapid and prohibits the use of elevated temperature processes for the formation of Ni-SiC whisker composites. The apparent difference between SiC whiskers and SiC filament with regard to reactivity with nickel is either a function of the character of the surface layer or a function of the fiber size with the high surface-area-to-volume ratio of the whisker contributing to its rapid dissolution.

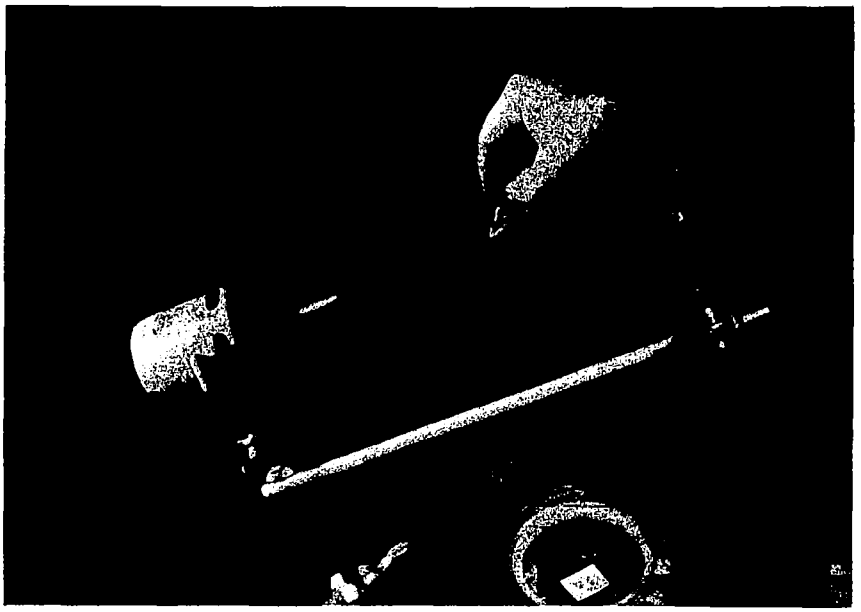

Figure 27. Mechanized Whisker Wire Spinning Apparatus

GTC 56-16

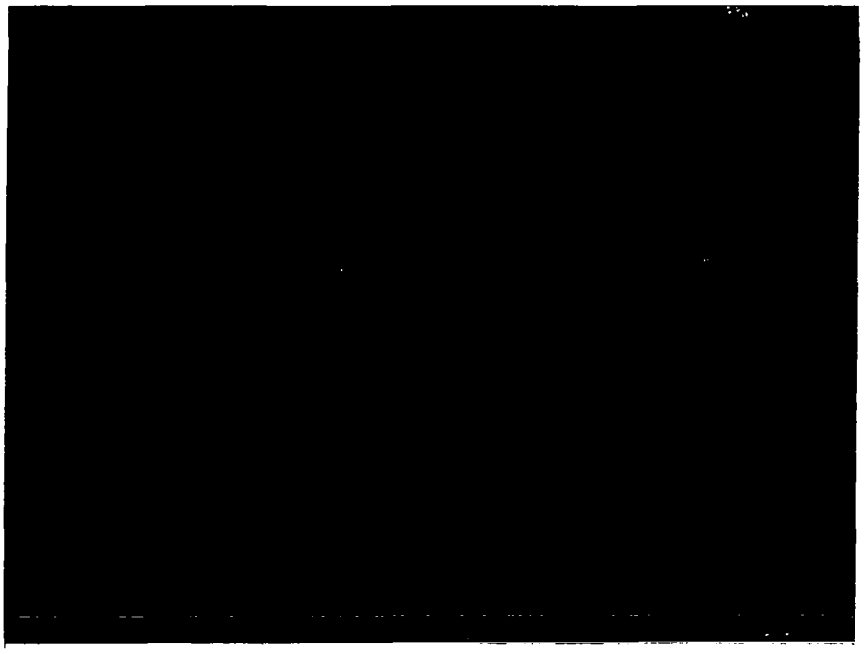

Figure 28. As Deposited Nickel Infiltrated Silicon Carbide Whisker Yarn 1500X

GTC 56-17

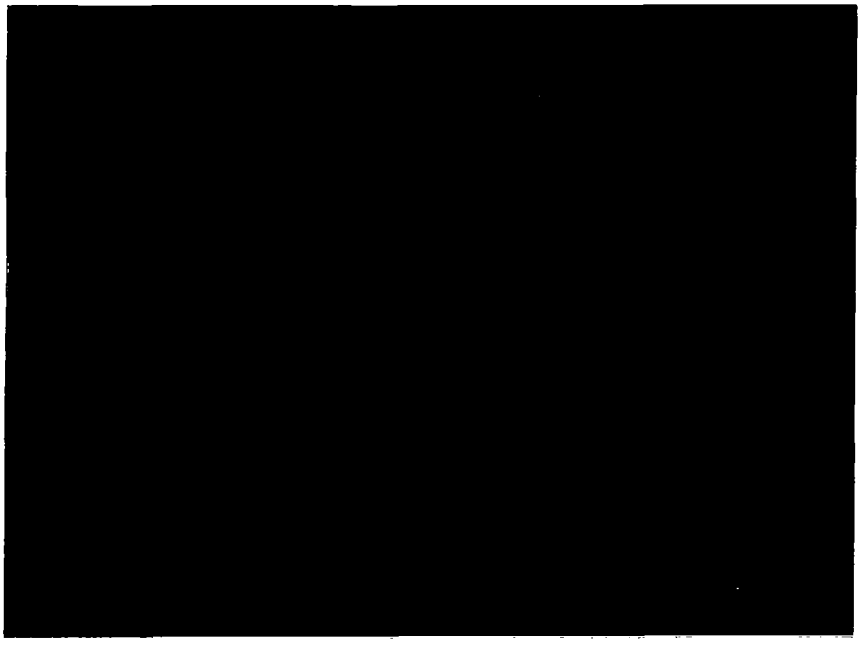

Figure 29. Nickel-Silicon Carbide Whisker Wire after 1 Hour at 700°C 1500X

GTC 56-18

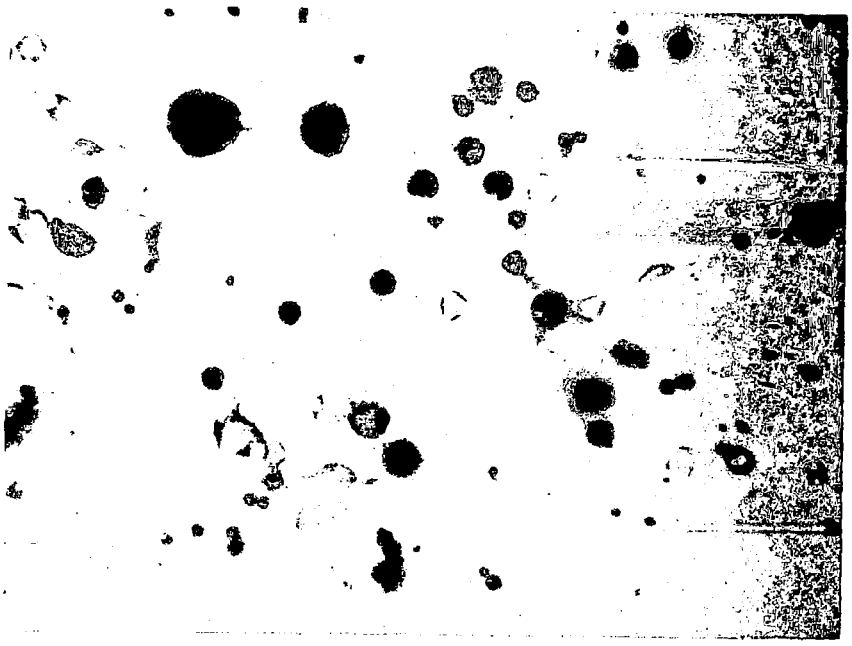

Figure 30. Nickel-Silicon Carbide Whisker Wire after 1 Hour at 800°C 1500X

GTC 56-19

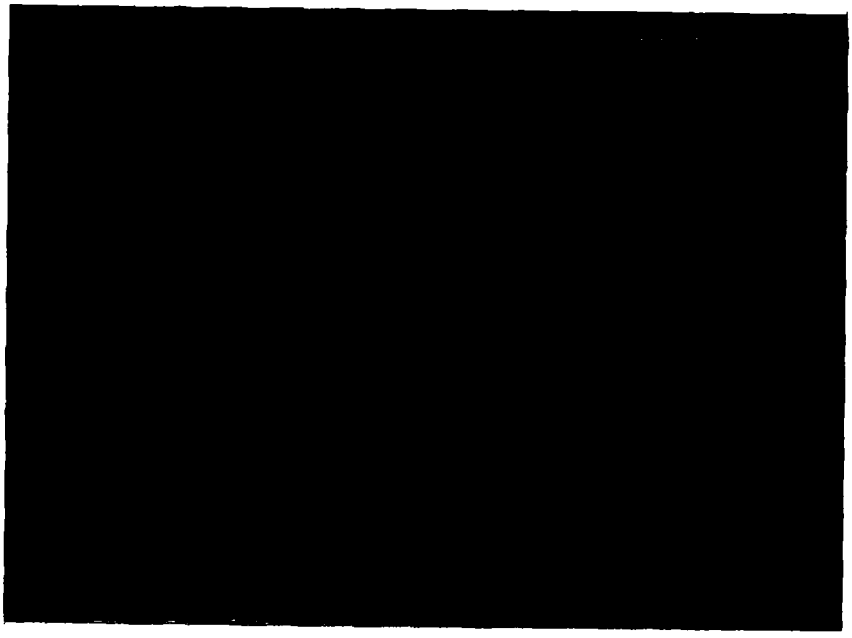

Figure 31. Nickel-Silicon Carbide Whisker Wire after 1 Hour at 900° C 1500X

The observation that elevated temperature reactivity was a problem with the Ni-SiC system was a severe blow to the planned fabrication of gross composite specimens for mechanical test within the scope of this program. The philosophy of the program, i.e., the accomplishment of whisker alignment, the infiltration of aligned whisker arrays and the mechanical testing of aligned whisker composites had been completed but the ability to utilize the aligned whisker wires to form gross composite specimens had not been demonstrated.

In an effort to accomplish that final objective, the whisker yarn infiltration effort was shifted to the aluminum matrix system and electrodeposition infiltration experiments were conducted to produce a whisker-matrix combination which could be fabricated into gross specimens by hot pressure bonding. Figures 32 and 33 show the surface structure of an aluminum infiltrated whisker yarn and the type of fracture observed on specimens fabricated in this manner. The extensive pull-out of whisker fibers at the fracture cross section and the low mechanical properties are recorded in Table 2. Time did not permit the development of the aluminum infiltration techniques to the stage exemplified by the nickel results. Experiments involving the systematic variation of deposition parameters to accomplish good fill and bonding would be advantageous.

The effort at GTC has added to the plethora of laboratory whisker specimens which have been fabricated and tested but these specimens (which have been exceedingly difficult to make) have shown that thousands of delicate whiskers can be incorporated in a matrix, properly aligned and bonded, and property determinations have indicated that their strengths are relatively unimpaired by the process. More important, the process for the accomplishment of alignment is based on a whisker fiber form which can be mass produced and is susceptible to scale by techniques analogous to textile manufacturing processes. The electrodeposition infiltration technique has been demonstrated for one metal system and preliminary work was conducted in another. The utilization of such infiltration processes are also susceptible to design for continuous operation offering the potential for producing in a wire form aligned whicker composites which can be used in secondary fabrication of gross composite parts. The specific reactivity of the particular whicker-metal combination concentrated upon this work should not detract from the demonstration which it provides.

Already the potential of the process developed here has excited interest in the easier resin infiltration of aligned whisker arrays. Preliminary results in that system are presented in Table 3 as an indication that even in matrices which are exceedingly weak good high strengths are attainable. The analogy between room temperature resin matrix properties and the elevated temperature properties of aluminum, for instance, would indicate that in a properly bonded and filled condition, aluminum matrix composites could exhibit high strength properties to within a few degrees of its melting point, a fact which is not insignificant in light of the requirements for skin and leading edge applications in supersonic aircraft. The philosophy of alignment, infiltration and utilization which permeates this work has generated activity at

GTC 56-20

Figure 32. Surface Structure Aluminum Electrodeposited on a SiC Whisker Yarn

GTC 56-21

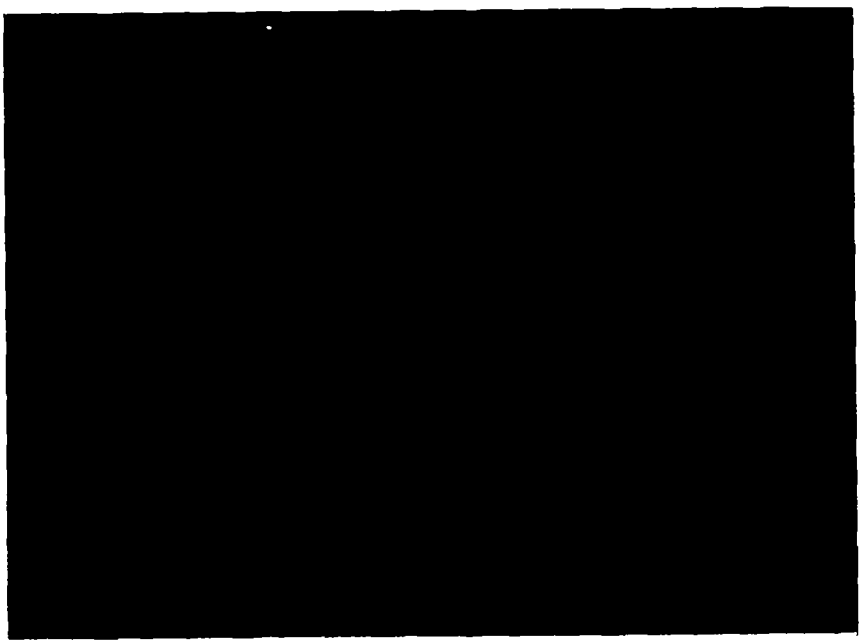

Figure 33. Fracture Motphlogy of an Electrolytically Infiltrated - Silicon Carbide Whisker Yarn

Table 2. The Mechanical Properties of Electrolytically Infiltrated Aluminum-Silicon Carbide Whisker Composites

Specimen No.	Tensile Strength (psi)
610	480
611	2400
612	7210

Table 3. Silicon Carbide Whisker Composite Data

Material Description	Tensile Strength (10^3 psi)	Modulus (10^6 psi)	Strength/ Density (10^6 psi)	Modulus/ Density (10^6 psi)
25 v/o whiskers in epoxy	126	30	2.2	520
10 v/o whiskers in nickel	226	44	0.8	150
10 v/o whiskers in soft glass	24	19	0.3	200
Conventional Materials:				
Isotropic E-glass in epoxy	144	4	1.9	52
7075 Aluminum	82	10	0.8	103
6 Al-4V titanium	155	15	1.0	94
Hastelloy X	114	29	0.38	97

Thermokinetic Fibers, Inc. which has yielded experimental sapphire whiskers in lengths which lend themselves to whisker yarn spinning and the vapor deposition capabilities of the GTC are being applied to the development of those techniques for aligned whisker array infiltration for matrices which cannot be electroformed.

CONTINUOUS FILAMENT REINFORCED COMPOSITES

Continuous filament reinforcement of metal matrices has been reviewed by Kelly and Davies[9] Cratchley[10], Machlin [14], and Rosen[35]. The treatments of the predicted behavior of continuous filament reinforced composites, their fabrication and the properties of experimental specimens are adequately described in those reviews of the field. Together with the report of previous GTC work, NASA CR-523 "A Study of Low Density, High Strength High Modulus Filaments and Composites"[36] they serve as a summary of the state of the art as it existed at the time this program was initiated.

The molecular forming process was utilized to prepare nickel matrix specimens reinforced with tungsten wire during the early stages of the program in order to develop the molecular forming process with a relatively inexpensive filament material and to provide specimens for comparison of the tensile and compressive properties of continuous filament reinforced sheet.

The electroforming technique for composite fabrication involves the electrodeposition of the matrix onto a suitable mandrel while concurrently winding the filament reinforcement and has been discussed by Bonnano and Withers.[37] A schematic of the composite fabrication process is shown in Figure 34. The technique is applicable to any metal that can be electrodeposited and has the following advantages:

1. It is a room temperature fabrication process.
2. A fully dense matrix sample can be concurrently deposited.
3. Intimate filament-matrix contact is accomplished at the interface.
4. Any shape which can be made as a surface of revolution can be fabricated.
5. Accurate control can be exercised over filament spacing and thus volume percent loading.

Figure 35 is a schematic of the growth pattern which is characteristic of this fabrication process. Figure 35A indicates the mode of formation of the electrodeposit on the filaments which are wound onto an undercoat of nickel on the winding mandrel. Figure 36 shows a monolayer nickel-tungsten tape formed in this manner. Figure 35B shows the continuation of the process by winding and coating of a second layer. Multiple layer samples are produced by a repetition of this process until the desired thickness is achieved. Figure 35C shows the location of potential void sites in the composite structure. Type 1 voids occur when deposition on the filament progresses at a rate such that the growth from two adjacent filaments intersects before growth from the undercoat reaches the point of intersection. Type 1 voids can be grown out at wide filament spacings by flooding the mandrel with fresh electrolyte and by the imposition of plate-deplate cycles on the forming operation. Type 2 voids are formed when the surface contour of the overcoat for the first layer does not conform to the filament size and shape. The character of such voids is shown in Figure 37. If the overcoat is thick enough the

GTC 56-50

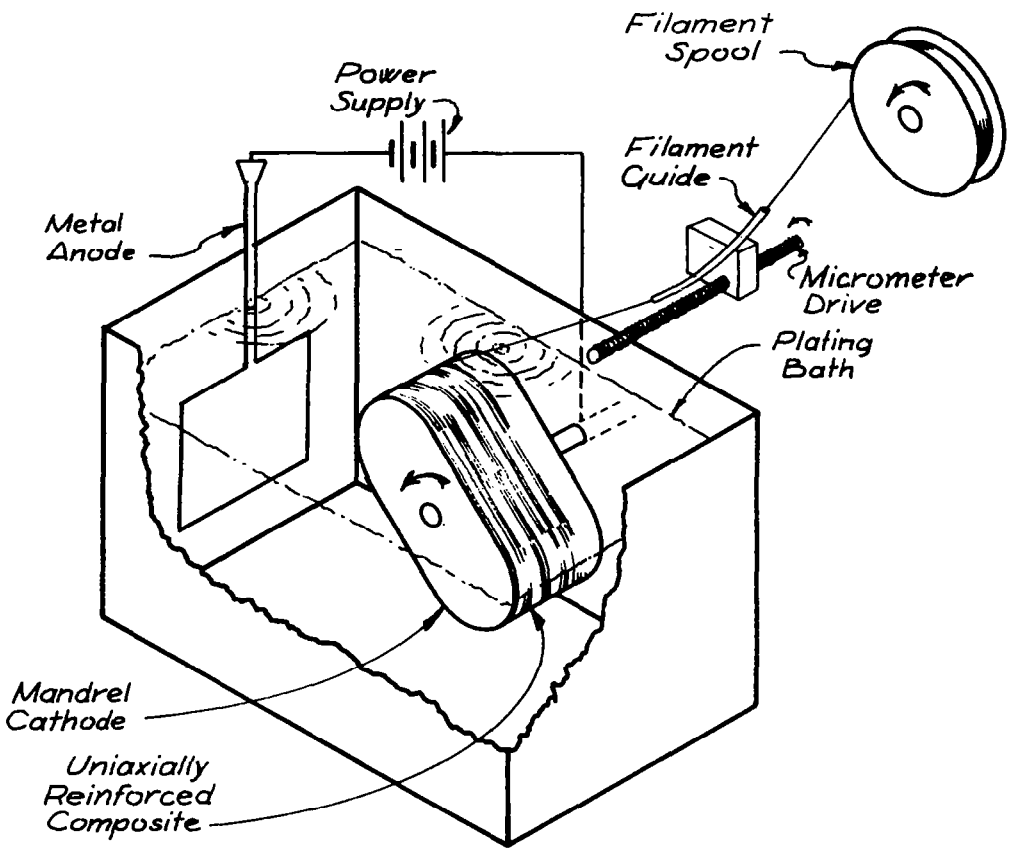

Figure 34. Schematic of Molform Process

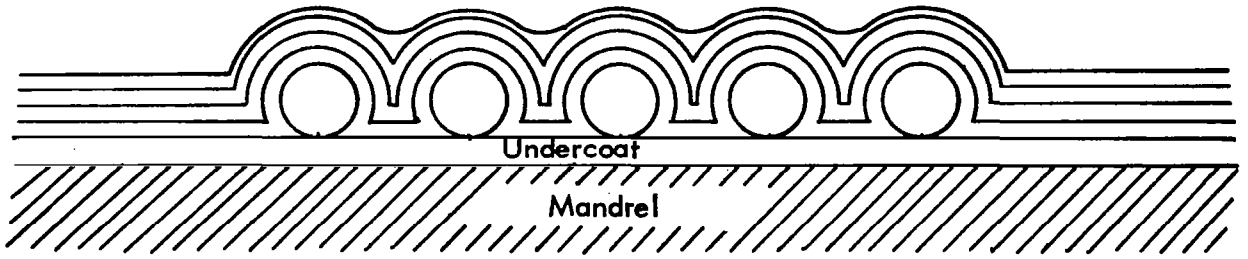

A. Monolayer Growth

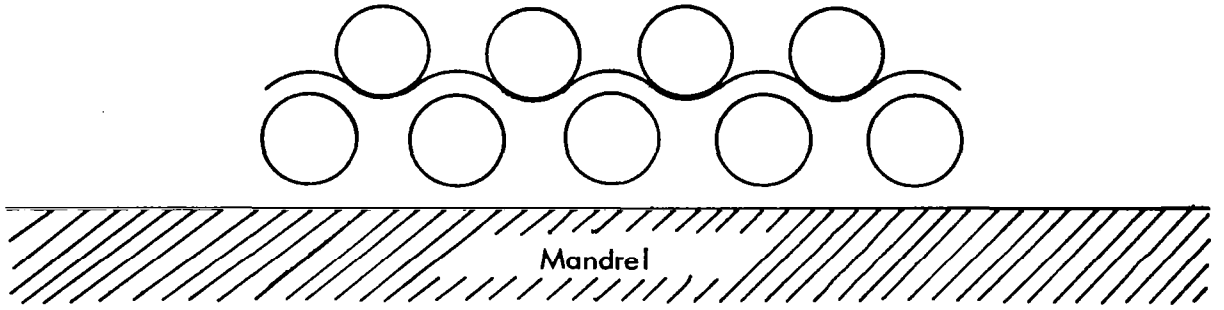

B. Multilayer Formation

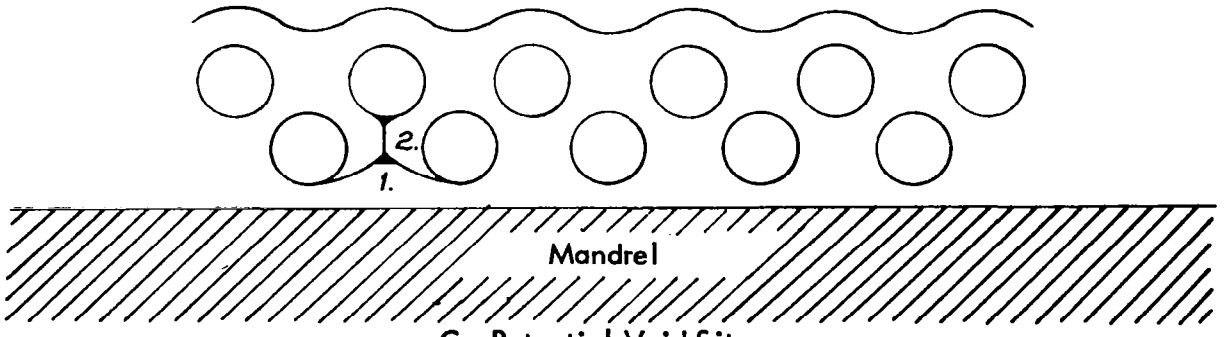

C. Potential Void Sites

Figure 35. Schematic Representation of Electroformed Composite Formation.

GTC 56-22

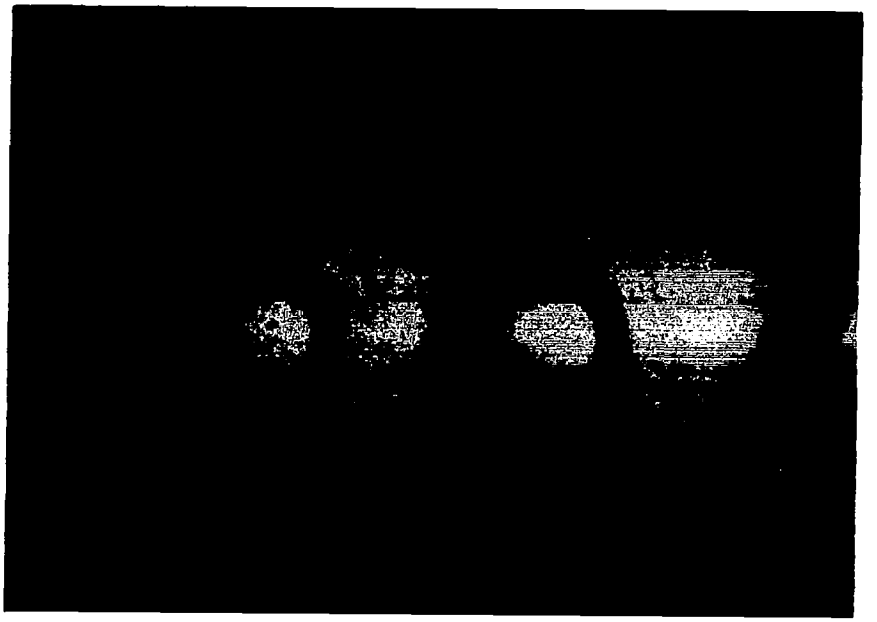

Figure 36. Monolayer W-Ni Composite Formed by Electrodeposition

GTC 56-23

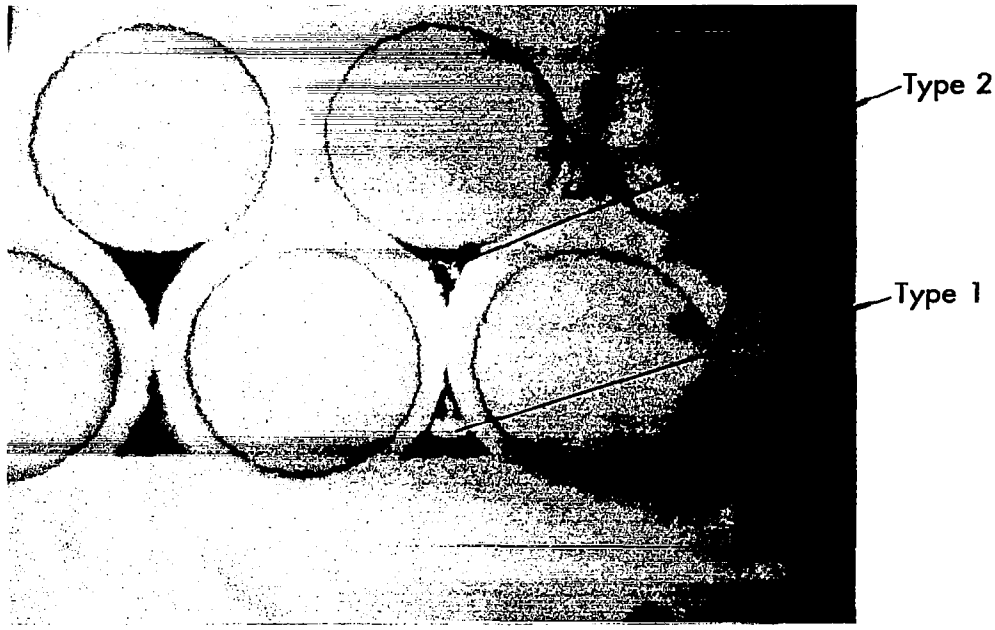

Figure 37. Void Formation in Ni-W Composites

grooves become rounded and accept the subsequent filament layer with little porosity. However, at high volume percent loadings the crevices occupied by the circular filaments leave triangular voids beneath them. It should be emphasized that even when the geometry of the surface is correct for the acceptance of the filament without void formation, the character of the bond between the filament and the matrix is different at the contact point than on the rest of its circumference. At that point it has simply been laid against the matrix, while elsewhere the matrix has been electrodeposited onto it. Another important consideration in the characterization of electroformed composites is the need for accurate control over filament spacing. Variations in filament spacings result in changes in the surface contour of the electrodeposited overcoat. Wide spacings yield a larger valley and close spacings create a larger hump and the effect of such misspacings is to force greater misspacings upon the subsequent layers. Such misspacings ultimately lead to a greater void formation in higher volume percent multilayered specimens. Figure 38 shows the effect of misspacings upon the distribution of filament in the composite and attendent void formation.

This effort characterizing the electroforming process for continuous filament reinforced composites can be summarized as follows:

1. Monolayer filament tapes can be produced with minimal void entrapment to roughly 40 v/o without elaborate plating innovations.
2. Multilayer composites can be formed to equivalent volume percent loadings but geometrical considerations combined with the potential for misspacings make void formation a problem to be contended with.
3. A densification process should be considered necessary in conjunction with composites formed by electrodeposition.
4. Monolayer tapes can be used as a raw material for multilayer composite fabrication by hot pressure bonding.

Tungsten filament reinforced nickel matrix composites fabricated by the molecular forming technique were prepared over the volume percent filament range of 0 to 52%. The mechanical testing of uniaxial tensile specimens cut from continuous filament windings was conducted and reinforcement behavior over the indicated range is tabulated in Table 4 . Figure 39 shows the tensile specimen configurations. The results of the mechanical testing program are plotted on a tensile strength and modulus versus volume percent filament basis in Figures 40 and 41 respectively. The law of mixtures line for each property is indicated in the figures. Measured values scatter about the law of mixtures lines. Values at higher volume percent loadings tend to fall below the line. At the lower volume percent loadings a significant number of results exceed law of mixtures values. At the higher volume percent loadings only the best specimens reach law of mixtures predictions. Attempts to molecularly form multilayer composites in volume percent loadings in excess of 52% resulted in a substantial fraction of void entrapment and such specimens were unsuitable for mechanical test.

GTC 56-24

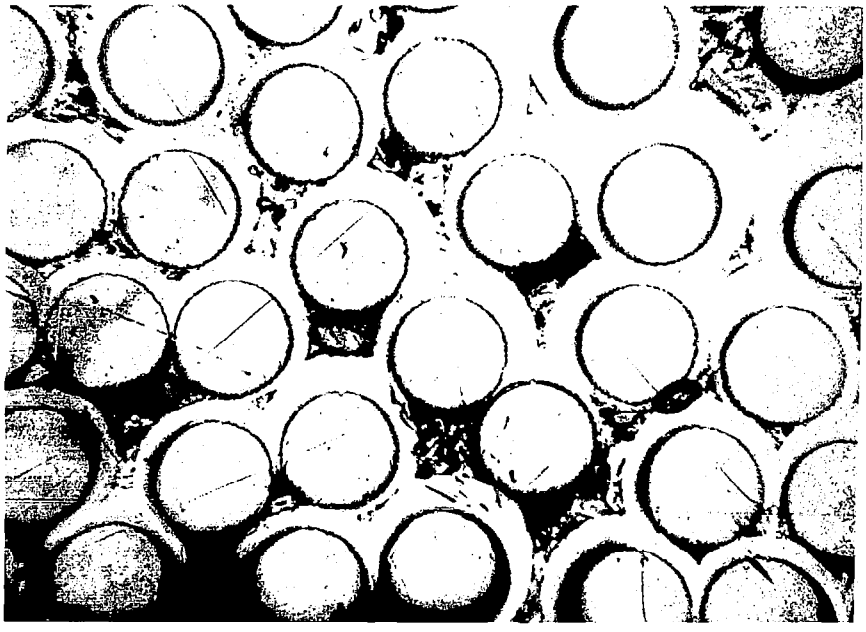

Figure 38. Multilayer Nickel-Tungsten Electrodeposition Infiltrated Composite 200X

Table 4. Tensile Properties of Tungsten Filament Reinforced Nickel Matrix Composites

Volume % Filament	Tensile Strength (10^3 psi)	Modulus (10^6 psi)
0	87.4	---
0	101.9	---
0	106.0	20.9
0	109.6	---
0	119.0	23.8
0	120.0	23.2
0	120.6	24.8
0	130.0	23.8
0	168.0	23.8
15.5	203.0	33.6
16	105.0	20.5
16	124.0	24.9
16	127.0	21.4
16	132.0	25.8
16	170.0	29.2
20	121.0	21.3
20	152.0	25.4
29.8	-----	28.4
29.8	-----	34.9
34.5	166.0	33.2
44.2	122.0	42.1
52	175.0	30.1
52.5	221.0	33.8

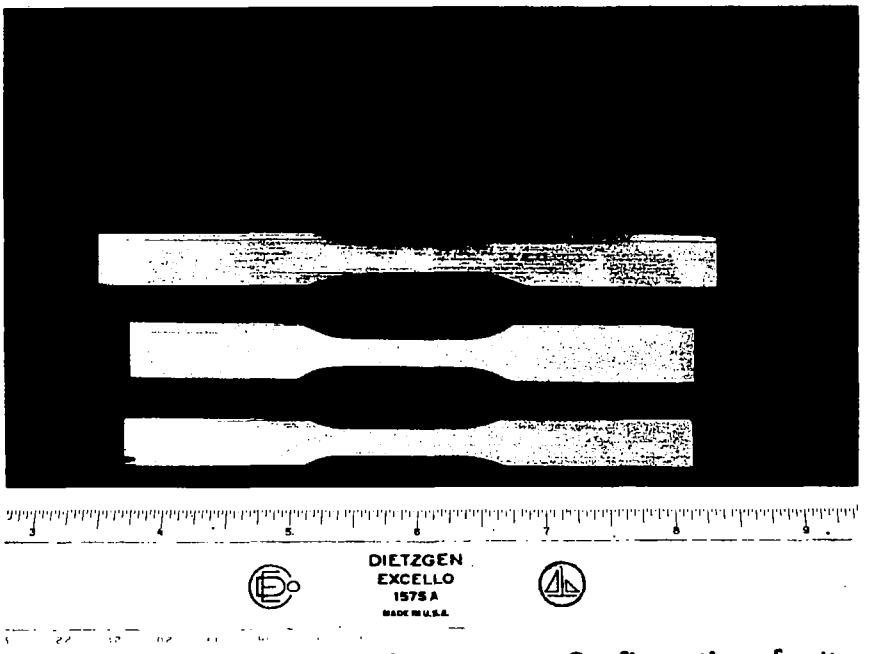

Figure 39. Typical Tensile Specimen Configurations for the Molecularly Formed Nickel Matrix Samples

GTC 56-51

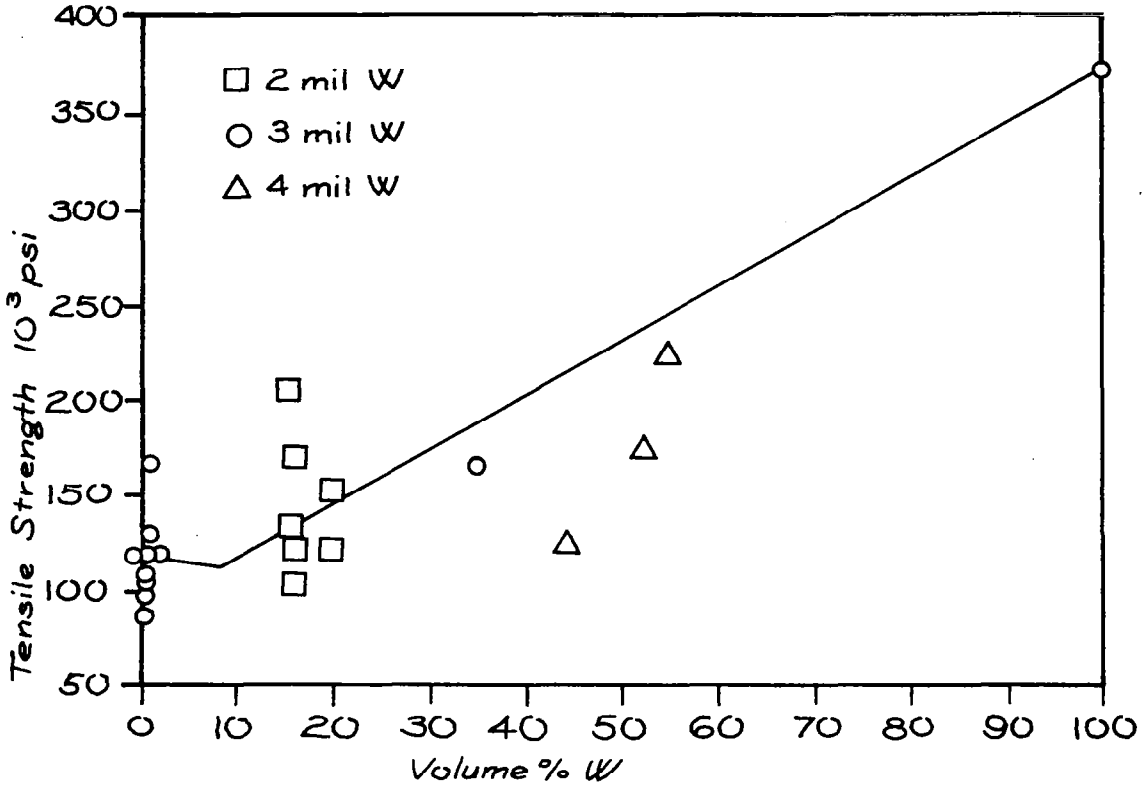

Figure 40. Tensile Strength versus Volume Percent Filament for Tungsten Wire Reinforced Nickel Composites

GTC 56-52

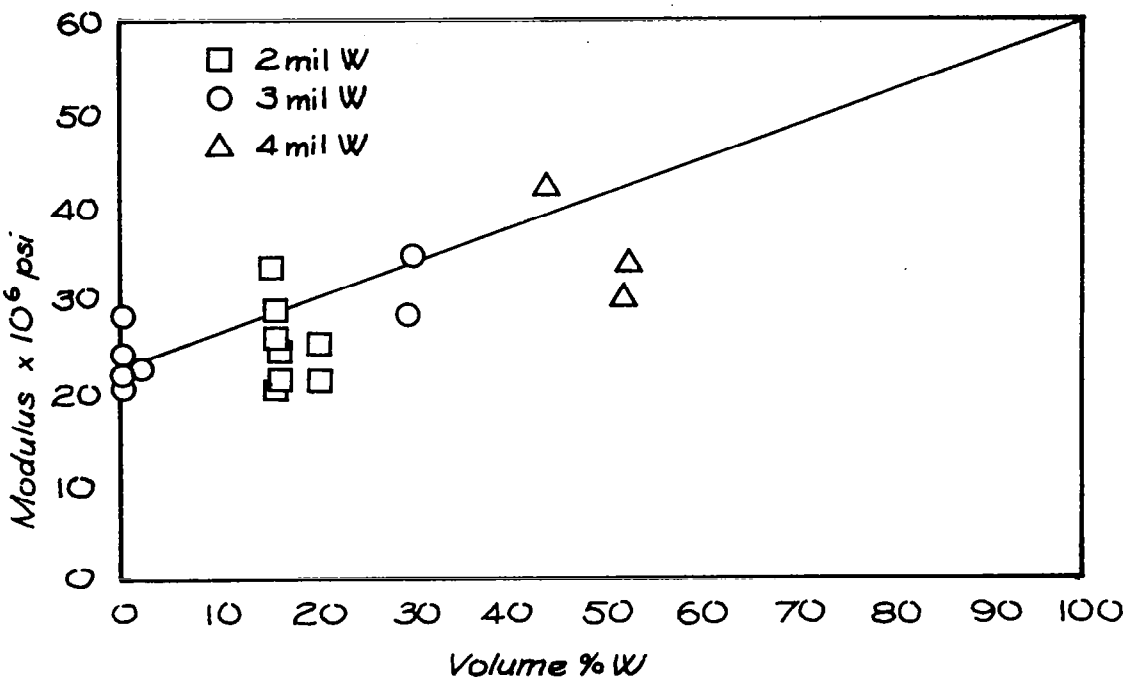

Figure 41. Tensile Modulus versus Volume Percent Filament for Tungsten Wire Reinforced Nickel Composites

The compressive properties of nickel-tungsten composites were measured following ASTM specifications for sheet specimens with a modified Miller-type support jig as shown in Figure 42. Initial attempts at compressive testing with relatively thin four layer composites resulted in repeated failures by bending of the short unsupported portion of the sheet specimen protruding from the Miller jig. The extent of protrusion was shortened and the specimen was fabricated with a two inch gauge length reduced cross section with a 2/1 ratio between the tab and reduced cross sections. Failure still occured at low stress and with low modulus by bending at the protruding end.

Nine layer composites were fabricated to yield a greater cross-sectional area and additional tests were performed. The results of compression tests on these thick sheet specimens are presented in Table 5 and the 35 v/o specimen is compared in properties with a tensile specimen cut from the same composite winding. The compressive strength and moduli values are quite low as measured by a test such as this. The conclusion of the effort on sheet specimen compression testing was that considerably thicker specimens would have to be fabricated to permit the testing of unsupported columnar type specimens.

Composite fabrication effort shifted at this point to the low density filament reinforcement boron in the light metal matrices aluminum and magnesium. The electrolytic deposition of aluminum from a lithium aluminum hydride, aluminum chloride, ether bath for protective coatings or electroformed parts was a commercial process at the GTC. The demonstration of aluminum electrodeposition as a molecular forming process for composites was accomplished at the GTC under contract AF 33(615)-3155 and a commercial apparatus for the fabrication of aluminum monolayer tapes was constructed. The aluminum tape fabrication apparatus is shown in Figure 43. The operation of the system is identical in principle to the procedure described for nickel, as shown in Figure 34, except for the fact that the aluminum bath must be enclosed in a dry box. Twenty five volume percent monolayer tapes were fabricated by electrodeposition in this apparatus and then cut to size and formed in a hot pressing die to yield twenty-layer-thick composites which could be utilized as free standing columns for compression testing. Figure 44 shows the filament distribution in a hot pressed composite formed from monolayer electrodeposited tapes. The compressive properties of free standing columnar samples of various lengths are presented in Table 6 . Specimens in excess of 3/4 inch in length failed at relative low strength values (less than the tensile strength of the composite). The strength recorded for the 1/2 inch specimens show marked increases in the compressive strength. The 114×10^3 psi value represents almost double the strength recorded in tension. Compressive modulus values are measured by crosshead motion and yield values that are essentially equal to the aluminum matrix modulus. Specimens were tested against tungsten carbide flats so penetration of the compression faces on the test apparatus is not a problem. In general, two types of failures were observed:

1. Delamination of the composite
2. Crushing at one end of the specimen.

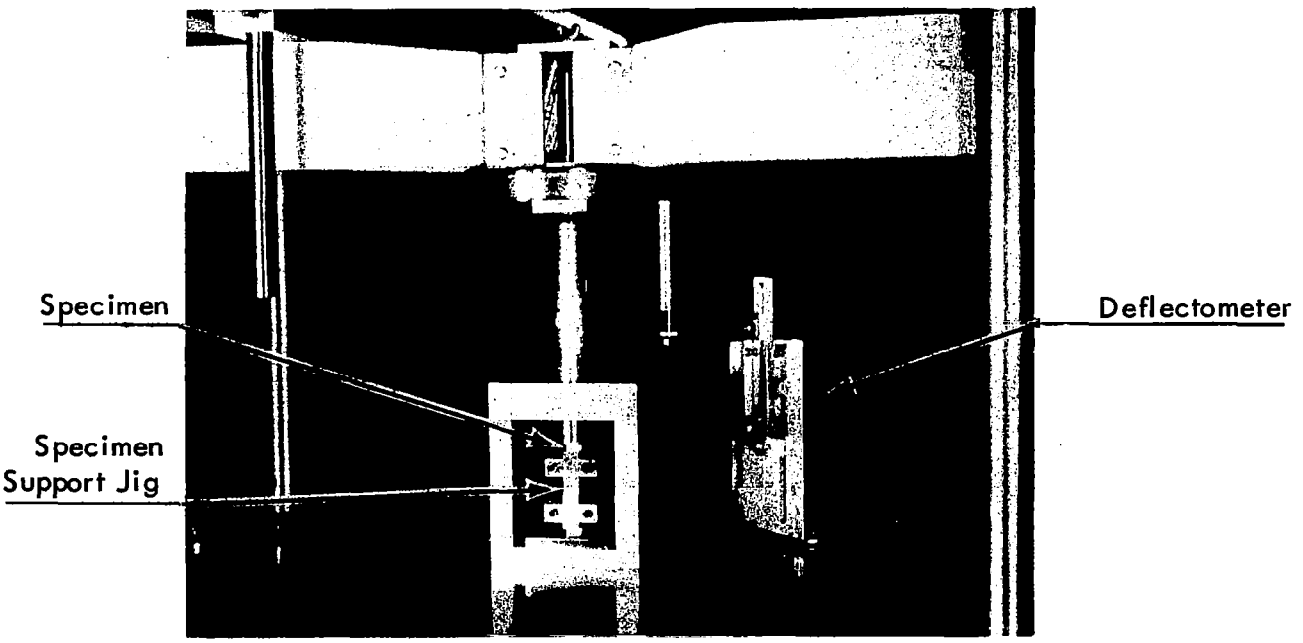

Figure 42. Compression Test Procedure for Sheet Composite Specimens

Table 5. The Compressive Properties of Ni-W Composites as Compared to the Measured Tensile Properties of Companion Samples

Specimen No.	Volume Percent	Tensile Strength (10^3 psi)	Compressive Strength (10^3 psi)	Tensile Modulus (10^6 psi)	Compressive Modulus (10^6 psi)
53-10A	35	166	136	33.2	18.4
53-10B	35		81		17.0
54-12	44		120		18.5

GTC 56-26

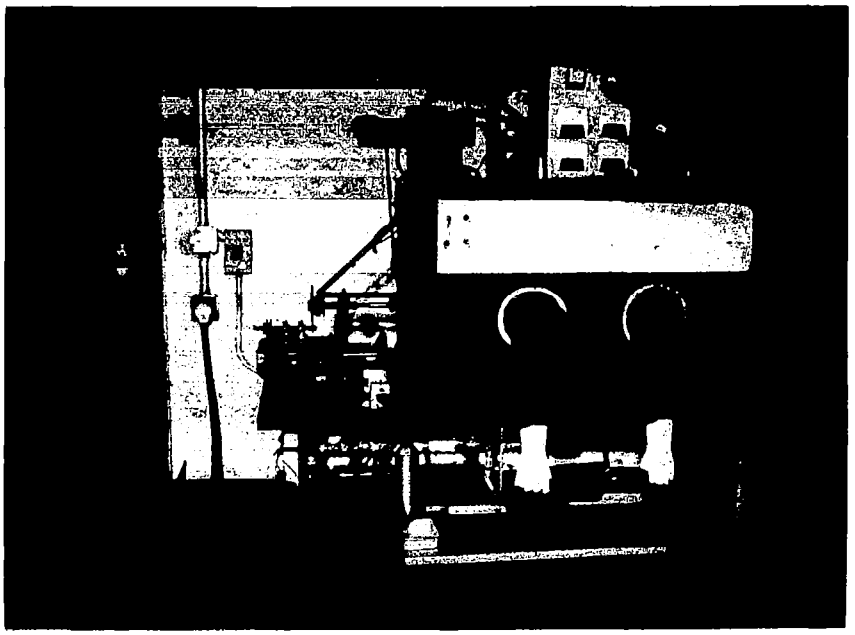

Figure 43. The Apparatus Utilized for the Electrolytic Fabrication of Aluminum Matrix Continuously Wound Composites

GTC 56-27

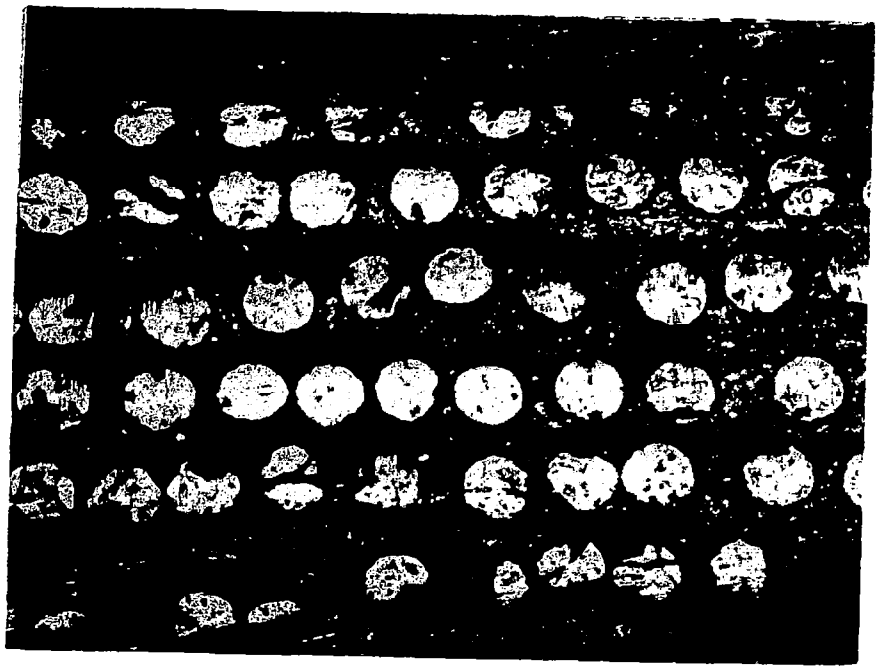

Figure 44. Hot Pressure Bonded Composite Specimen Format from a Stacked array of Electrolytically Deposited Monolayer Tapes 100X

Table 6. Compressive Properties of a 25 v/o Boron-Aluminum Composite Having a Tensile Strength of 58.9×10^3 psi and a Modulus of 22×10^6 psi

	Specimen Length (Inches)	Compressive Strength (10^3 psi)	Compressive Modulus (10^3 psi)
IV A-1			
a		37.1	8.84
b	1 1/4	25.4	4.18
c		20.7	----
IV A-2			
a		Split End No Load	----
b	1	46.0	9.78
c		5.7	3.29
IV A-3			
a		44.4	8.67
b	3/4	20.4	6.20
c		31.8	9.64
IV A-4			
a		80.8	7.62
b	1/2	93.4	8.30
c		114	8.61

*Modulus is based on crosshead motion.

Failures occured by buckling at one end or by splitting of the column.

Delamination was associated predominantly with the low compressive values, while the highest strength specimens showed only the end-crushing phenomenon.

Attempts to make 1/4 inch circular cylinders of Al-B by liquid metal infiltration were not successful. Molten aluminum reacts with boron to form an aluminum boride layer at the interface as shown in Figure 45. Coating of the filament with nickel was indicated by DeLai[38] to provide some short time protection from aluminum boride formation. A coating apparatus, Figure 46, capable of continuous electrolytic deposition of nickel onto boron was used to coat filament with a thin layer of metal for subsequent infiltration. Figure 47 shows the interface between nickel coated boron and liquid metal infiltrated aluminum with no evidence of filament reaction at the infiltration temperature of 700°C for 10 minutes. While reaction could be subdued in liquid infiltration experiments, the degree of fill accomplished was not outstanding and thus mechanical tests were not accomplished on liquid metal fabricated cylindrical specimens.

Liquid metal infiltration was observed to be more complete and reproducible in the Mg-B system without reaction at the interface. High volume percent filament specimens could be fabricated. The compressive strengths of a series of cylindrical specimens are presented in Table 7. Composite specimen JM44 was tested between hardened steel plates and the reinforcing filaments were distinctly embedded into the plates during testing. The resulting exceedingly high compressive strength value for this specimen must be attributed to this case where substantial end constraint is applied to the specimen. The balance of the specimens for which volume percent calculations have been made were tested against tungsten carbide plates with no indication of indentation of the pressure application plates. Specimens 8M6 and 5M represent very attractive compressive strength properties for the volume percent loadings present in those samples. All of the moduli values are extraordinarily low. Again moduli are determined by crosshead motion but the recorded values range from 1/2 to 1/4 of the tensile modulus values observed at those volume percents. All of these specimens failed by buckling or crushing at one end. Failure modes are exemplified by the photographs in Figures 48 and 49. The remaining series of specimens listed in Table VII failed by single or multiple splitting of the cylinder. As shown in Figure 50 this is indicative of poor infiltration.

Both magnesium and aluminum matrix composites can be formed by hot pressure bonding in an apparatus which is shown in Figure 51. Foils are placed in the two flat faces of the winding-pressing mandrel and a layer of filament is wound onto the mandrel in spaced array. A second foil layer is added to each flat face and another layer is wound. This process is continued until the desired number of layers are formed and a final foil is over the last filament layer. The wound mandrel is then positioned between the two heated platens, brought to temperature and hot pressed. A pressure of 9000 psi at 500°C for one hour was found to be adequate to form well consolidated composite plates such as is shown in Figure 52.

GTC 56-28

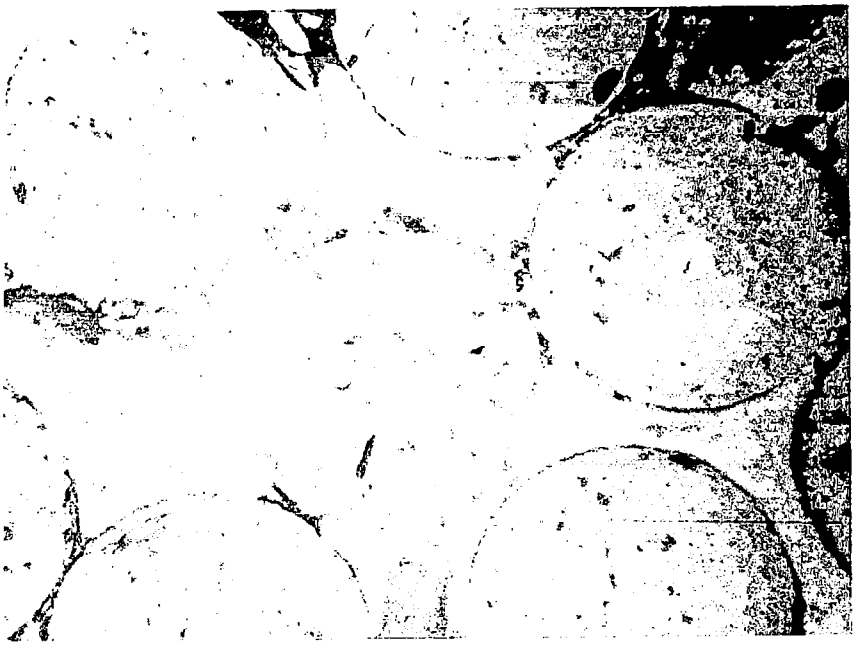

Figure 45. Aluminum Boride Formation at the Interface During Liquid Metal Infiltration of Boron Filament arrays at 700°C for 10 minutes 400X

GTC 56-29

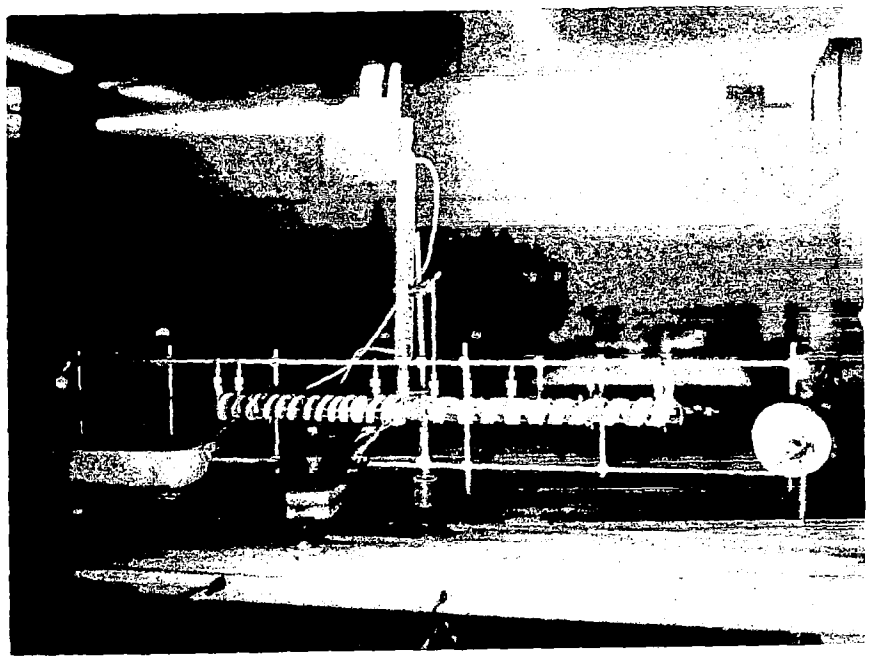

Figure 46. Continuous Filament Electrolytic Coating Apparatus

GTC 56-30

Figure 47. Liquid Aluminum Infiltrated Nickel Coated Boron 800X

Table 7. Compressive Properties of Boron-Magnesium Cylindrical Compression Specimens

Specimen No.	Volume Percent	Compressive Strength (10^3 psi)	Compressive Modulus (10^6 psi)
JM44	69.0	457	20.6
8Md	46.7	131	9.5
8Mc	46.7	141	11.6
8Mb	46.7	236	8.7
8Ma	46.7	113	8.4
7M	37.2	133	9.2
5M	35.0	299	12.1
6M		65	6.6
3		49	6.4
2		70	6.4
1		60	3.8

GTC 56-31

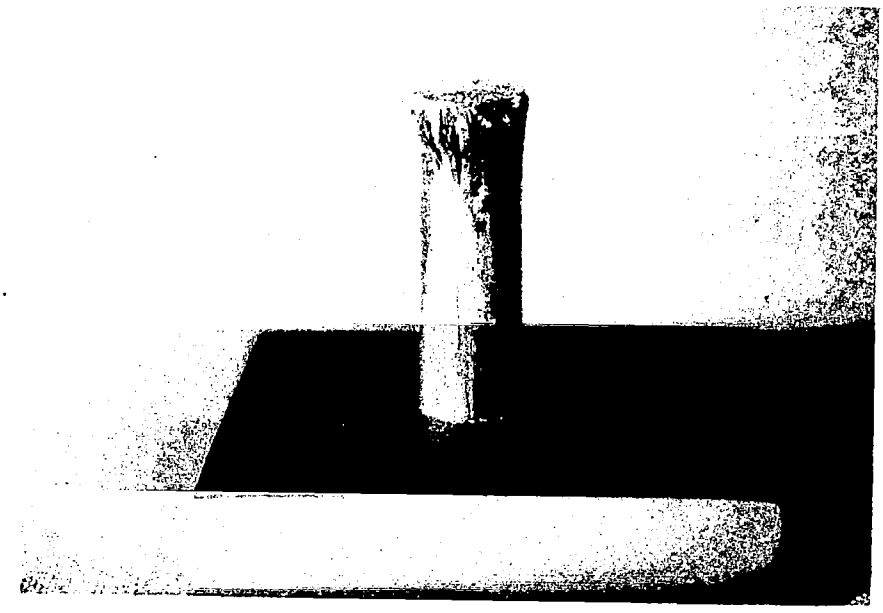

Figure 48. Accordion End Failure in a Boron-Magnesium Compression Specimen

GTC 56-32

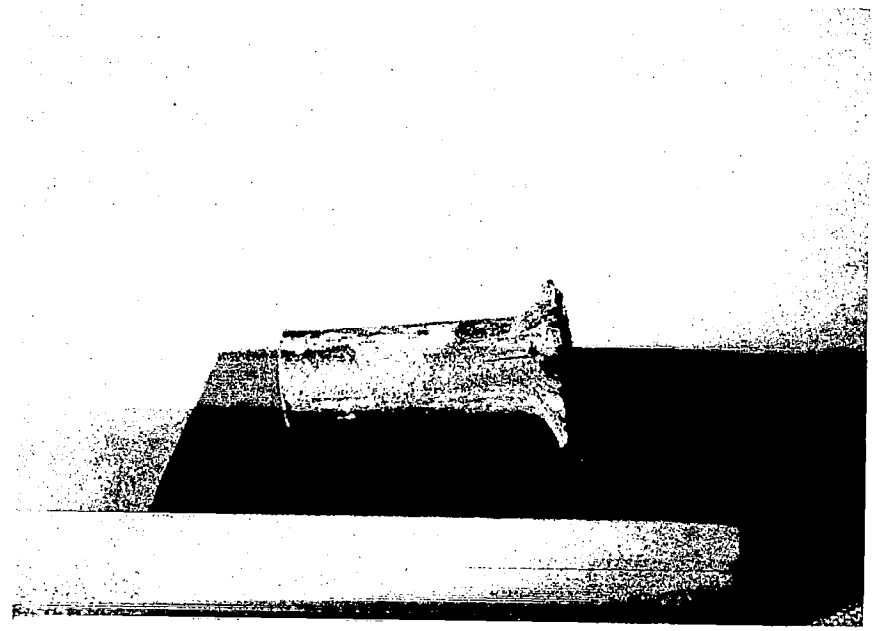

Figure 49. Mushroomed End Failure in a Boron-Magnesium Compression Specimen

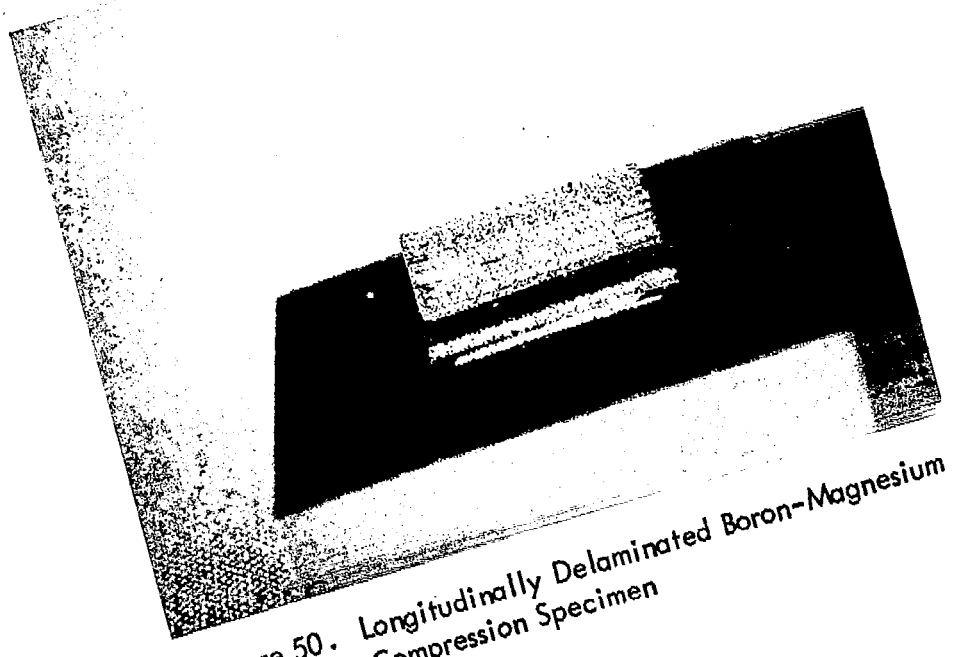

Figure 50. Longitudinally Delaminated Boron-Magnesium Compression Specimen

GTC 56-34

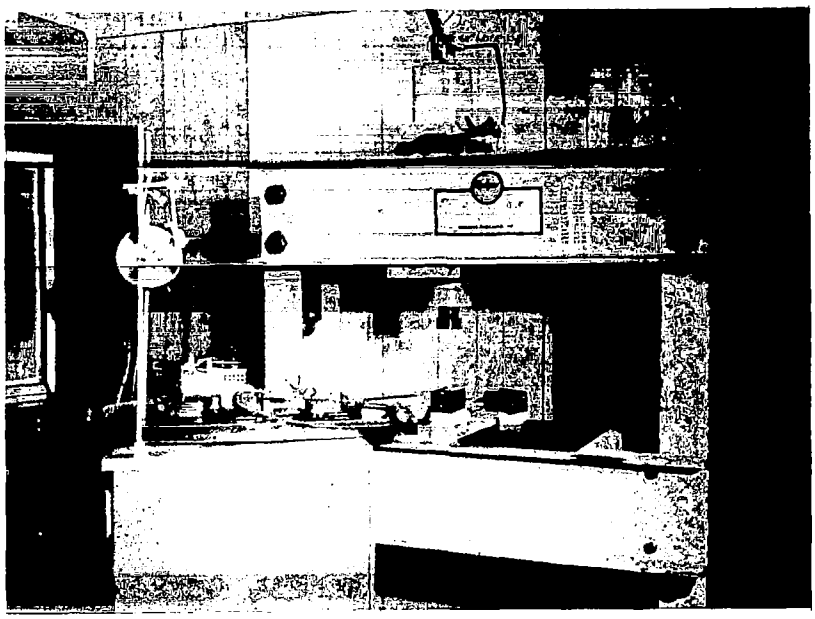

GTC 56-35

Figure 51. The Hot Pressing Apparatus Utilized to Form Hot Pressed Composites from Metal Foils and Continuously Wound Filament Arrays

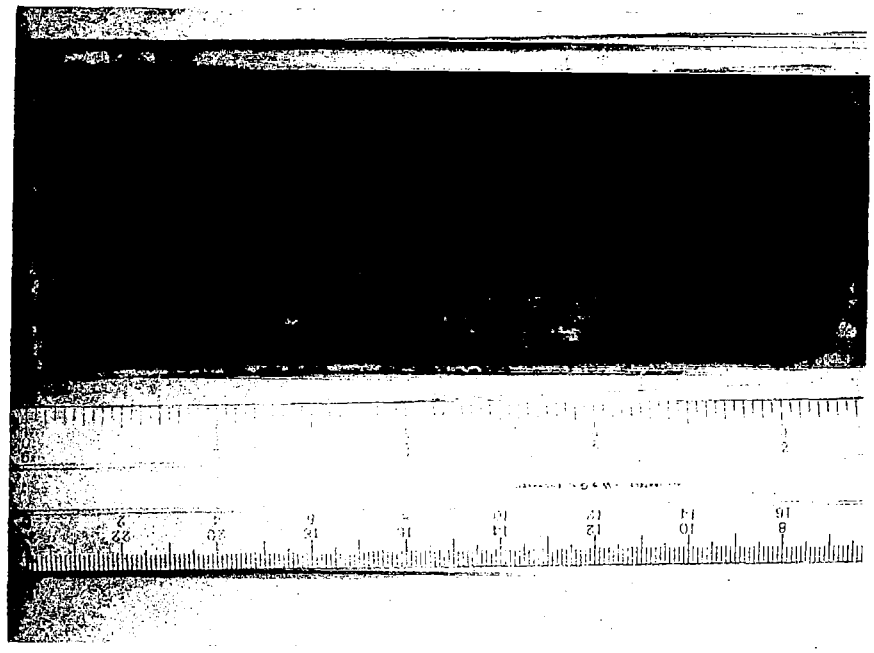

Figure 52. A Mg-B Composite Panel Fabricated by Hot Pressure Bonding of Continuously Wound Filament Foil Arrays

Specimen panels with 35 v/o filament were fabricated in this fashion and were cut into a series of tensile and flexure specimens for test at a series of span-to-depth ratios. Flexure strength values were determined in three point bending as shown in Figure 53.

The flexure and tensile strength results on these series of samples are shown in Table 8. The moduli values in flexure are observed to be roughly 60% of the tensile values on the same composite and among the moduli values the higher span-to-depth ratio specimens yield consistently high values. No such span-to-depth correlation seems to exist with the flexure strengths. Strength values are observed to range from about 130% to in excess of 200% of the associated tensile values.

Very little compressive and flexure testing had been accomplished on metal matrix composites at the time that this program was initiated. Schuerch[39] had reported results on two compression specimens and a bend specimen. Compression strengths of 188×10^3 psi and 344×10^3 psi for magnesium composites with 52% and 71% filament respectively were measured. A flexure strength of 199×10^3 psi in three point bending for a 52 volume percent specimen was also reported. No moduli values were reported. Anelastic crippling failure was evaluated according to the shear crippling theory for a simplified composite model in that report. The predicted and experimental values for compressive strength vs. packing density for the GTC work and that of Schuerch [39] are presented in Figure 54. Recently Kreider [40] has reported that flexure modulus values for Al-B composites in four points bending are in the same range with tensile values. For the system Al-Be, Sinizer [41] has reported that compression and tensile yield strengths are nearly equal while the compressive modulus appears to be less than the tensile modulus. Results for the system Ti-B by the same investigators indicate that both modulus and yield strength values agree in tension and compression.

In this work the compressive strength and modulus of nickel-tungsten composites were both lower than tensile values for the same specimens. For the aluminum-boron system compressive strengths twice the tensile values were accomplished while compressive moduli were barely one third the tensile values. For magnesium-boron composites compressive strengths two to three times the tensile values were observed while modulus values were as low as observed for the aluminum-boron system. Flexure strength values in the magnesium-boron system were as high as twice the tensile values while moduli values were down by one third.

These observations do not represent a coherent picture because of the differences in the composite system investigated, the specimen configuration utilized and the method of test performance. Superimposed upon these gross differences are the internal variabilities within any one system or fabrication technique. Concentrated effort on one system and fabrication technique with standardized test techniques would permit the broad interpretation of the various test results and serve as a basis for a comprehensive understanding of composite behavior as exposed to simple states of stress.

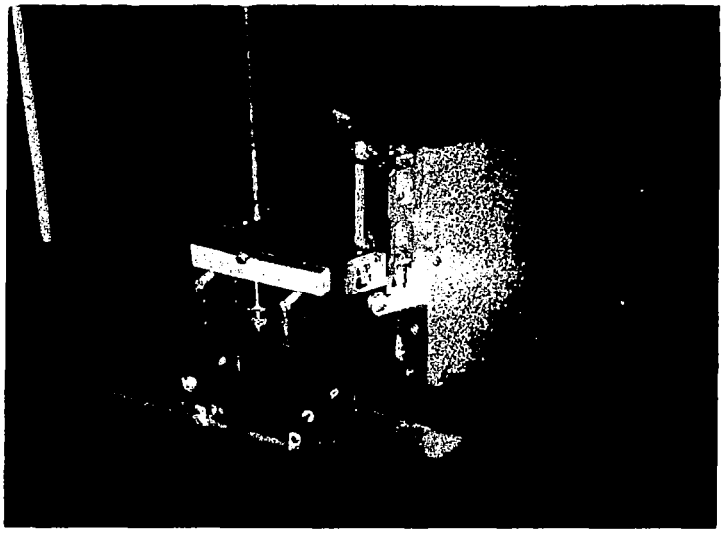

Figure 53. Three Point Bending Apparatus with Deflectometer

Table 8 . The Flexure Properties of 35 v/o B-Mg Composites with Various Span-to-Depth Ratios as Compared with Tensile Properties

Specimen No.	Type of Test	Span: Depth	Strength $\times 10^3$	Modulus $\times 10^6$
41	Tensile		59.2	26.4
42	Flexure	77:1	81.9	17.5
42 A	"	35:1	86.5	16.3
42 B	"	35:1	87.4	16.0
43	"	75:1	109	16.8
43 A	"	35:1	110	15.0
43 B	"	35:1	109	14.5
44	"	75:1	96.7	17.0
44 A	"	35:1	96.9	15.1
44 B	"	35:1	110	14.0
61	Tensile		53.9	26.5
62	Flexure	100:1	112	18.8
62 A	"	35:1	114	16.2
62 B	"	35:1	103	17.1
63	"	75:1	98.4	16.4
63 A	"	35:1	97.5	16.5
63 B	"	35:1	79.5	15.8
64	"	75:1	116	18.1
64 A	"	35:1	117	16.9
64 B	"	35:1	104	16.6
31	Flexure	35:1	49.1*	13.1
32	"	35:1	37.0*	8.64

*Shear Failures

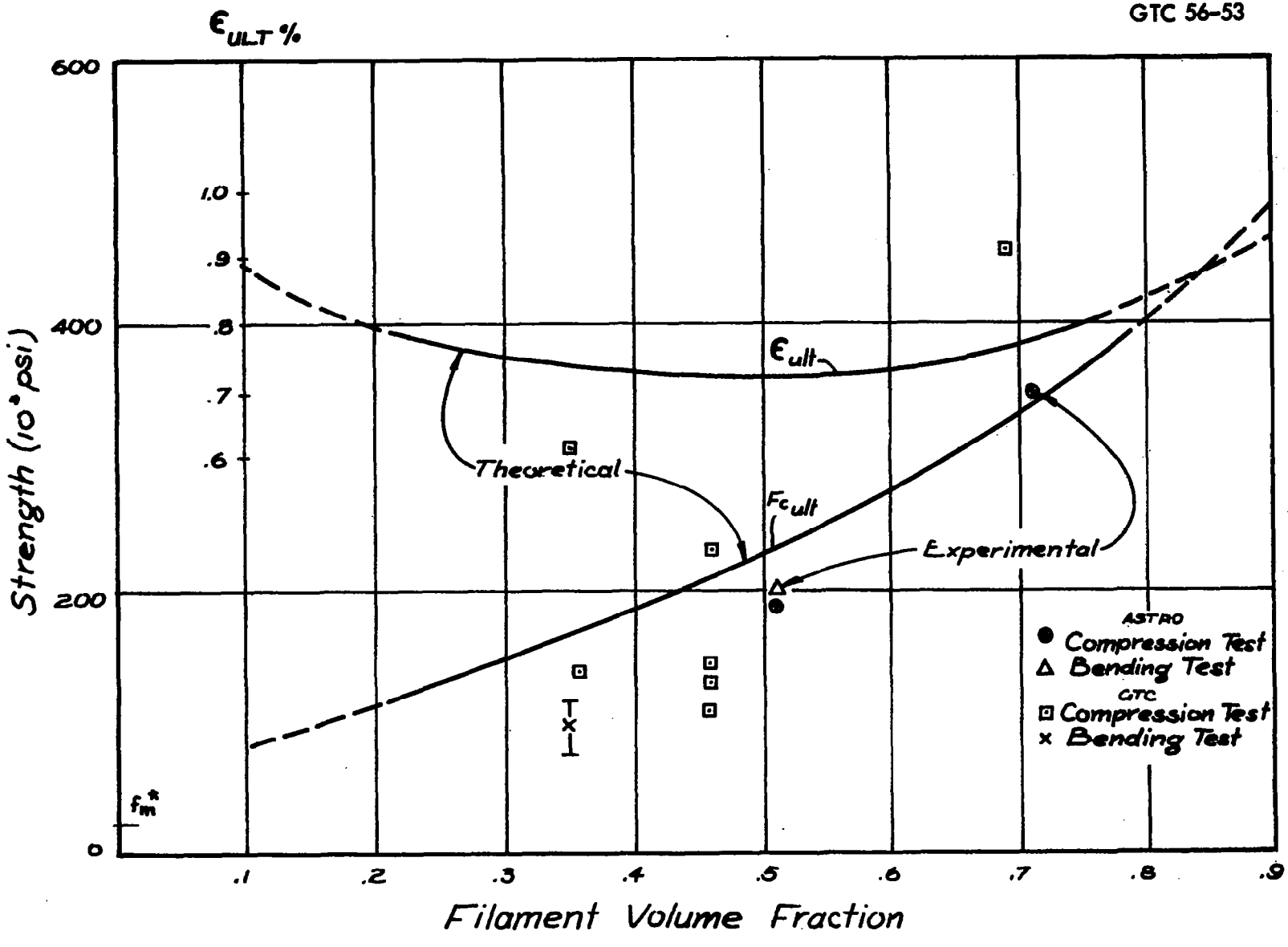

Figure 54. Predicted and Experimental Strength vs Packing Density for B/Mg Composites.

The attractiveness of the magnesium-boron system as a model ceramic filament-metal matrix composite is emphasized by the extraordinarily good compression strengths recorded for that system in this report. Magnesium forms a strong interfacial bond with boron without compound formation or extensive filament degradation. It is the only structural metal that can be formed into a high quality composite by liquefaction techniques and in other sponsored work at GTC (AF 33(615)-3155), its strength-to-weight performance in tension has exceeded 1.2×10^6 inches, with a modulus-to-density ratio of 425×10^6 inches.

A patent disclosure is currently being drafted for submission to the Assistant General Counsel for Patent Matters, NASA, Washington, D. C., concerning the continuous casting of Mg-B rod by the drawing of a close packed array of boron filaments through a liquid magnesium bath. The product of such experiments is shown in Figures 55 and 56. Such a process can be envisioned as being immediately capable of providing rods of various diameters for use in space vehicle application requiring such high strength-to-density and modulus-to-density ratios. The extrapolation and scale-up of such a process to yield high quality structural plate for noncorrosive environment application is considered to be practical.

GTC 56-37

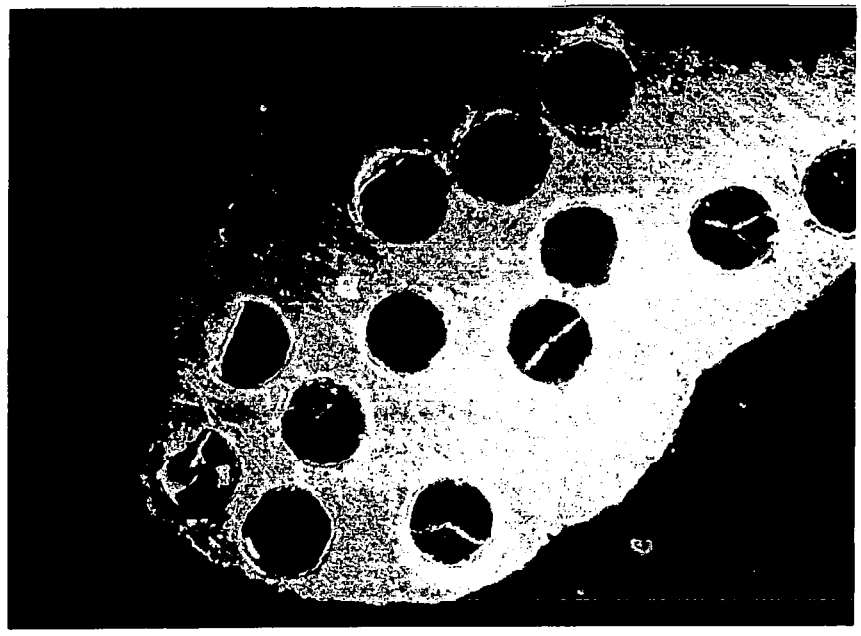

Figure 55. Low Volume Percent Boron-Magnesium Composite Formed by Continuous Casting

GTC 56-38

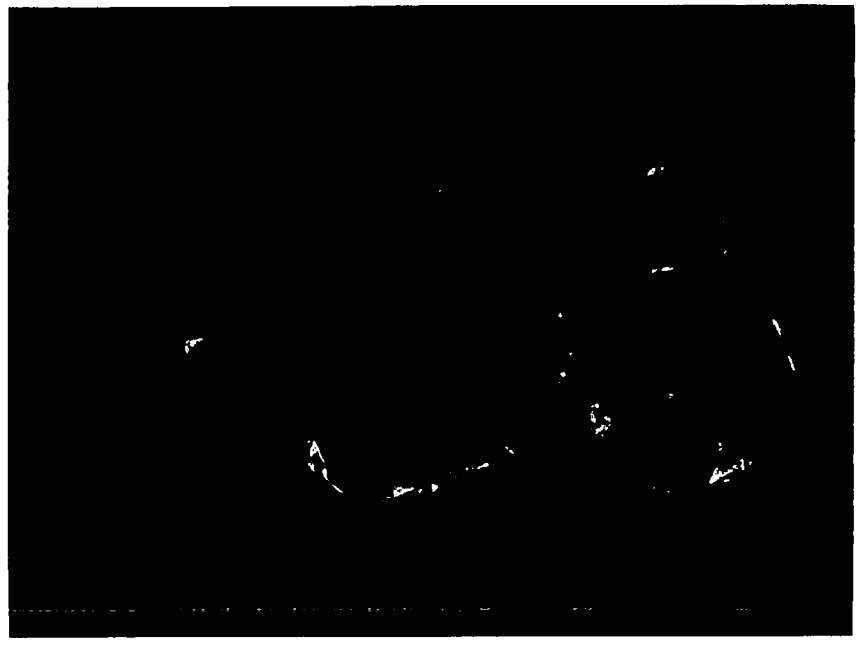

Figure 56. High Volume Percent Boron-Magnesium Composite Formed by Continuous Casting

MULTILAMINAR METAL-CERAMIC COMPOSITES

Multilaminar metal-ceramic composites were first proposed by Shanley[42]. The concept of these materials was developed in an effort to overcome the inherent brittleness of cermet materials. Ductility in metals results from slip on close-packed planes in the individual metal grains. The simple combination of metal and ceramic powders to form a cermet does not impart significant ductility because deformation in the metal grains must be accompanied by deformation in the ceramic grains. The construction of a multilaminar metal-ceramic composite which could be crushed into pseudo grains and reconstituted as a cermet with metallic slip planes included in each grain should yield a cermet material with improved room temperature ductility. Attempts to produce such composites of flame-spraying techniques demonstrated the principle, but the morphology of the early specimens indicated that the lamellae were not as planar as was desired. The investigation of such composite fabrication by vapor deposition techniques was recommended.

For the multilaminar composites work conducted under this program, the system Mo-TiB_2 was chosen as a materials combination because of NASA Langley Research Center interest in molybdenum as a structural material and because titanium diboride has a close thermal expansion match with molybdenum over the temperature range utilized in the vapor deposition process.

Based on continuous filament development effort at GTC, the reactants titanium tetrachloride, boron trichloride and hydrogen with argon as a carrier gas were proposed for the formation of TiB_2 layers while molybdenum was to be deposited from a molybdenum hexafloride-hydrogen mixture. The objectives of the program were:

1. The determination of the deposition conditions for accomplishing the individual deposits,
2. The determination of the best substrate for the initial deposited layer and the means for releasing the laminar composite from the substrate,
3. The determination of procedures for obtaining maximum adhesion between the individual layers of the composite,
4. The deposition of bi-layer composites, and
5. The deposition of multiple layer composites and mechanical testing.

The dual train laminar composite deposition system is shown schematically in Figure 57. The deposition substrate is mounted in the reaction chamber and is heated by induction. The temperature is monitored with a thermocouple and the substrate is brought to reaction temperature in argon. Then the desired ratio of reactant gases were admitted to the chamber at constant flow rates. When the first constituent has been deposited, the reactant gases are shut off and the temperature changed to the reaction temperature for the second constituent and the second set of reactant gases are admitted. Various modifications of the deposition procedure are described in the discussion of experimental results.

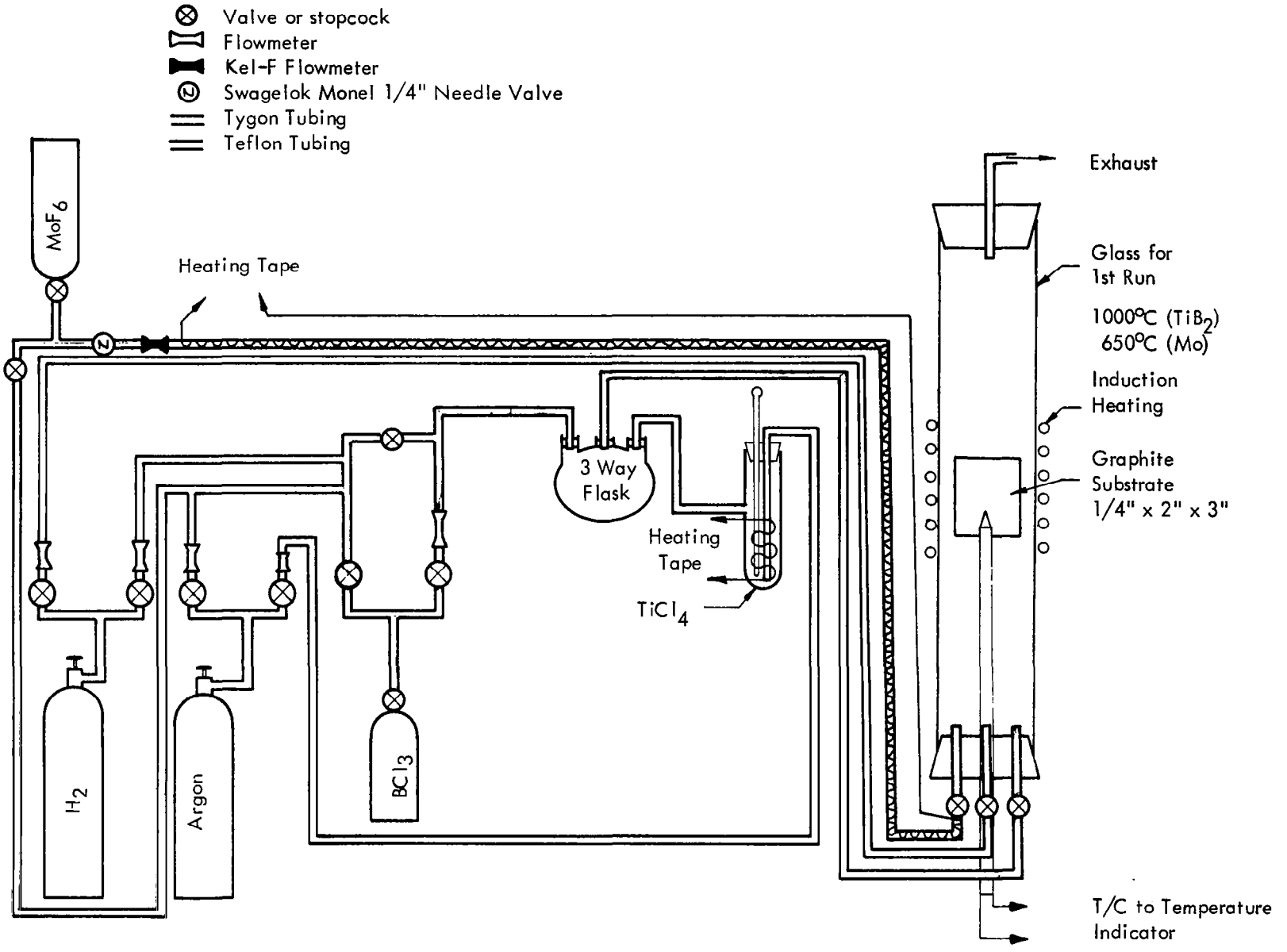

Figure 57. Apparatus for Laminar Composite by Alternate Vapor Deposition of TiB_2 and Mo onto Graphite Substrate.

The deposition temperatures for TiB_2 were varied between 950°C and 1090°C with the range from 1050°C to 1090°C yielding the best deposits. Molybdenum was deposited between 655°C and 880°C with 850°C yielding the best deposits.

Considerable difficulty was experienced in developing a procedure which would give good adhesion between the deposit and the molybdenum foil substrate and between deposited layers. No problem was experienced in accomplishing adhesion to a graphite substrate. It was found that improved adhesion to molybdenum foil could be obtained if a thin layer of vapor deposited molybdenum was first deposited to the foil. It was also found that adhesion could be improved between molybdenum and a titanium diboride if the temperature of the sample was maintained while the deposition gases were being changed.

Figures 58 and 59 show typical molybdenum-titanium diboride deposits obtained from these experiments. Figure 58 shows molybdenum-titanium diboride deposited on molybdenum foil. While the layers are quite uniform, delamination occurred along the interfaces. Such delamination was characteristic of samples which were permitted to cool between depositions. Figure 59 shows a similar composite on graphite. Good adhesion between the layers is apparent. However, the surface of the graphite causes a somewhat roughened deposit. The layers in this picture were taken at an oblique angle which exaggerates their thickness. The nickel overlayer was an electrodeposit to maintain the deposit edges in metallographic preparation.

The results of the deposition experiments are summarized in Table 9 and represent the development of the deposition parameters for the individual constituents, for bilayer composites and for multilayer growths. Figures 60 and 61 show two multilayer Mo-TiB_2 deposits which indicate the character of the deposits which could be formed. The absence of interlaminar crackingis an indication that good bonding was accomplished and that residual stresses resulting from the relatively low thermal expansion mismatch are not sufficient to cause delamination.

Figure 62 is a further illustration of the interlaminar adherence. In this photograph fractures induced in attempts to strip the deposit from the graphite substrate cross the interfaces between lamellae without delamination.

The utilization of vapor deposition techniques for the formation of multilaminer composites has been successfully demonstrated as feasible for the system Mo-TiB_2 in this work. The reconstitution of laminar composite deposits was not accomplished within this program since effort during the final quarter of work was concentrated on the generation of mechanical property data in both the whisker and filament reinforced composite areas. Sufficient time was not available for the development of the reconstitution procedures and the mechanical testing of generated samples. However, process development experience inherent to the deposition experimentation did permit the design of a deposition chamber adequate to produce gross quantities of

GTC 56-39

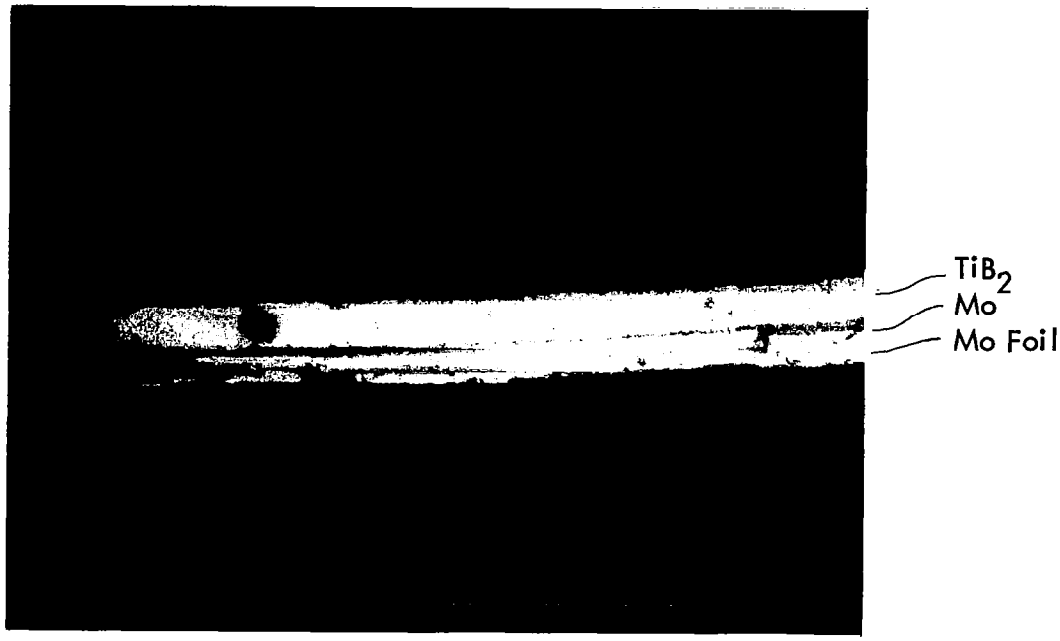

Figure 58. Mo and TiB_2 Vapor Deposited onto a Molybdenum Foil Substrate 400X

GTC 56-40

Figure 59. Mo and TiB_2 Vapor Deposited onto a Graphite Substrate 200X

Table 9. $Mo-TiB_2$ Multilayered Composite Deposition Studies

Sample No.	TiB_2	Mo	Substrate	Comments
III-A-1	1020	-	Graphite	1-2 mil coating, X-ray TiC
III-A-2	1000	-	Mo foil	Coating flaked off
IIIA-3	1002	-	Mo foil	Coating flaked off
IIIA-4	1010	660	Etched Mo foil	TiB_2 flaked, Mo spotty
IIIA-5	1075	-	Etched Mo foil	TiB_2 good adhesion
IIIA-6	950	655	Etched Mo foil	Coatings flaked
IIIA-7	-	665	Graphite	System leaked
IIIA-8	970	700	Etched Mo foil	Adhesion between coatings poor
IIIA-9	1050	-	Electropolished Mo foil	Coating flaked
IIIA-10	1050	850	Graphite	Good bilayer coating
IIIA-14	1050	850		
	1085	825		
	1090	850	Graphite	Good multilayer coating
	1050	835		
		835		
IIIA-15	1050	850		
	1090	865		
	1080	880	Graphite	Good multilayer coating
		870		
IIIA-16	1050	850		
	1060	850	Graphite	Good multilayer coating
IIIA-17	1050	850		
	1090	850	Graphite	Good multilayer Coating

GTC 56-41

Figure 60. A Seven Layer Mo-TiB_2 Composite

GTC 56-42

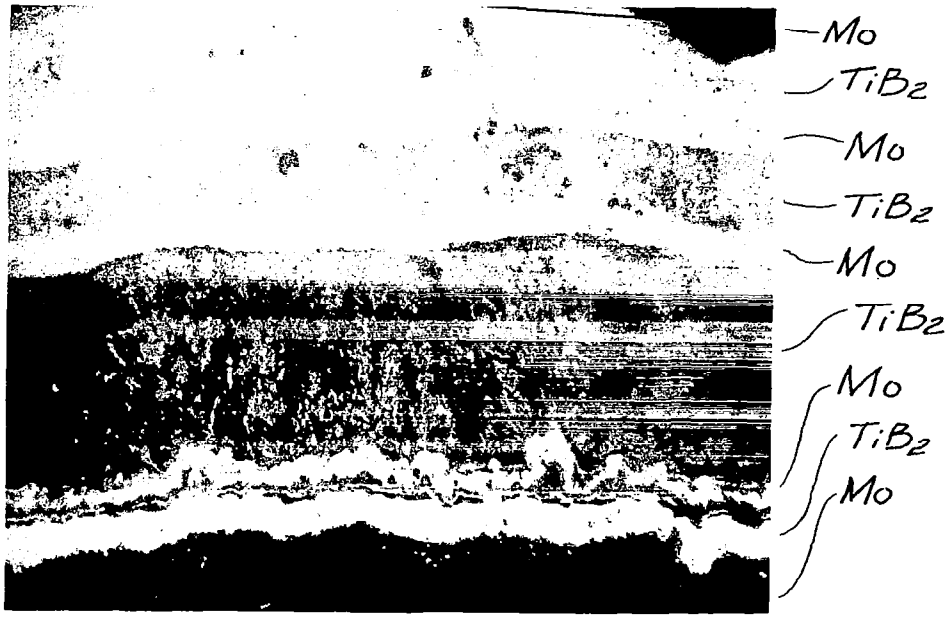

Figure 61. A Nine Layer Mo-TiB_2 Composite

GTC 56-43

Figure 62. Fracture baths crossing Lamellae Interface without Delamination

vapor deposited Mo-TiB_2 or other selected constituent composites for reconstitution and mechanical testing. A schematic of that system is shown in Figure 63. A graphite or metal reaction tube is heated by induction to the reaction temperatures for the two constituents. Thermal cycling and gas switching can be accomplished automatically. The deposit would be circular but lamellae would essentially be planar when crushed to a small grain size for reconstitution as a cermet.

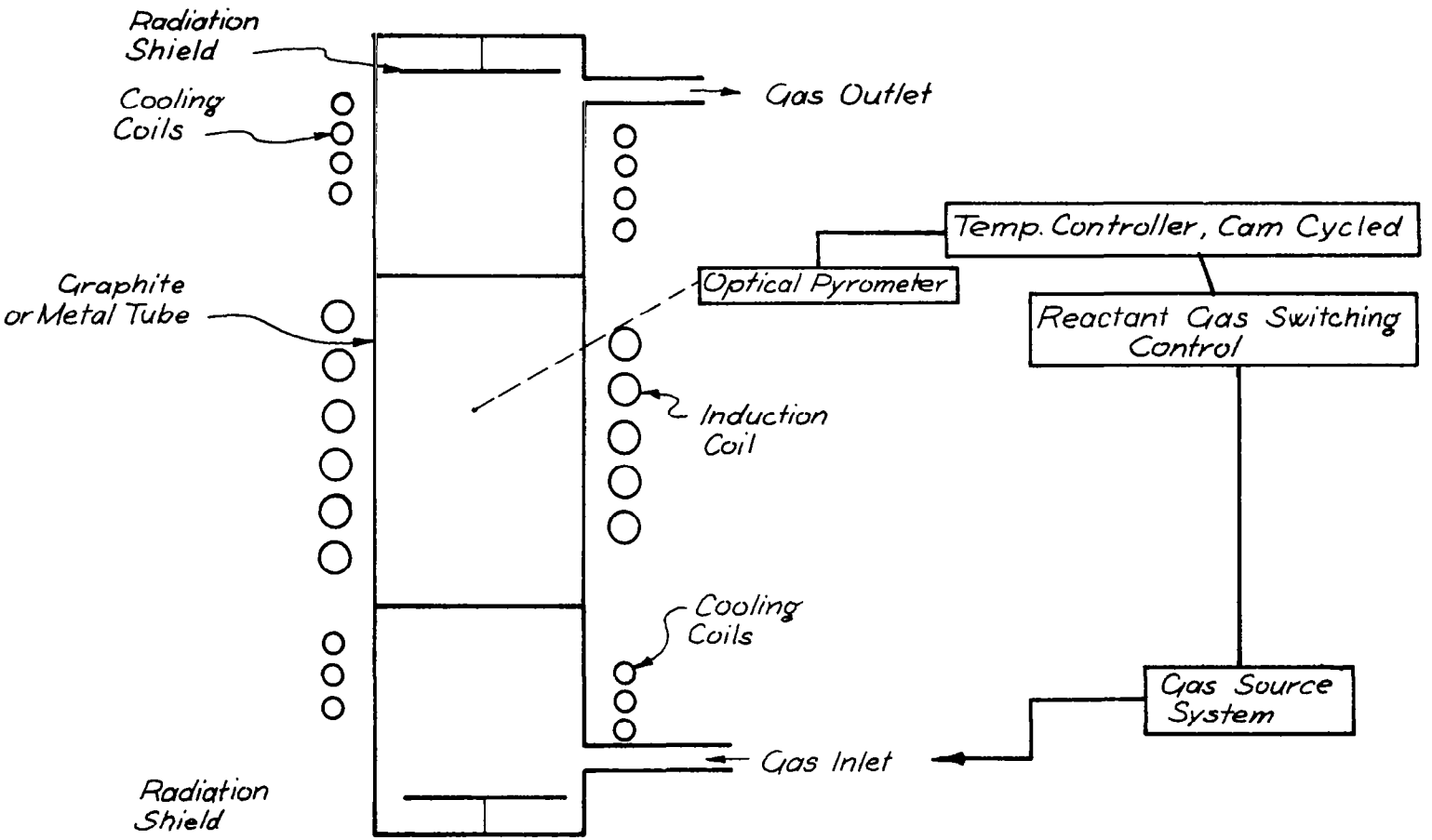

Figure 63. Schematic of Prototype Production Unit for Multilaminar Composite Fabrication.

CONCLUSIONS AND RECOMMENDATIONS

The first objective of such a broad survey-type program should be the provision of focus for future efforts in the various areas studied. The specific accomplishments of the program on whisker, filament and multilaminar composites can be summarized as follows:

1. Molybdenum and titanium diboride can be deposited by vapor deposition techniques in multilaminar form with good adhesion between the two materials.
2. Electro forming, electroforming plus hot pressing, foil-filament array hot pressing and liquid metal infiltration have been examined as filament composite fabrication techniques and the strengths and weaknesses of the various systems enumerated.
3. The tensile, compressive and flexure properties of Ni-W, Al-B and Mg-B filament reinforced composites have been compared.
4. The Mg-B filament reinforced system has yielded exceedingly high tensile and compressive strength values and is observed to be characterized by a good filament matrix bond with little filament degradation even when fabricated by liquid metal infiltration techniques.
5. A textile spinning alignment procedure for long SiC whiskers has been developed and shows promise as a production technique for the accomplishment of high volume percent aligned whisker arrays.
6. Infiltration of aligned whisker arrays by electrodeposition of nickel into spun SiC whisker yarns has been accomplished.
7. Nickel infiltrated aligned SiC whisker wires have been mechanically tested and have demonstrated strengths which indicate whisker strength utilization in excess of 1 million psi.

The conclusions and recommendations which evolve from the accomplishments of this program for the three areas of composite materials surveyed are as follows:

1. Multilaminar Composites
   a. Vapor deposition is a practical technique for forming multilaminar composites
   b. Its feasibility in specific systems is dependent upon the ability to develop and maintain a good interlaminar bond between the two phases.
   c. Molybdenum and TiB_2 have shown good adherence and therefore can be recommended as a model system.

d. Scale-up of experimental deposition systems should be accomplished to yield sufficient material for reconstitution in the form of bulk specimens for mechanical test.

2. Filament Composites
   a. The best filament reinforced composite materials are the product of a fabrication technique which permits the assembly of the filaments and matrix in a fashion so as to minimize degrading reaction between the constituents while maximizing the interfacial bonding between them.
   b. Electrodeposition fabrication techniques are applicable to any metal or alloy which can be electrodeposited and have the advantages of being low temperature fabrication processes which put the matrix in intimate contact with the filament, can provide fully dense composites under controlled conditions and can yield a concurrently generated metal sample closely simulating the actual matrix in the composite. The technique is limited by the requirement for extremely accurate filament spacing tolerances, the occurrence of void formation at high volume percent loading and the increasing potential for fault formation with increasing numbers of filament layers. The most promising product of the electrodeposition technique is the monolayer tape which can be fabricated as a precursor for gross composites formed by hot pressure bonding techniques.
   c. Hot pressure bonding was utilized in conjunction with both Al-B and Mg-B systems and yields good quality composite specimens. Good filament matrix bonding is achieved in the Mg-B system at all temperatures between 500°C and 600°C while over the same range adherence is accomplished only at the higher temperature in the Al-B system. Higher fabrication temperatures in the Al-B system result in lower composite strengths, indicative of the potential degrading reaction at those temperatures.
   d. Liquid metal infiltration is quite successful with the magnesium matrix while aluminum boride formation is observed in similarly fabricated aluminum matrix composites.
   e. Fabrication development and composite property optimization should be accomplished in both the Al-B and Mg-B systems. Because of its natural tendency to form high quality composites by both hot pressure bonding and liquid metal infiltration, the Mg-B composite system should be utilized as a model metal-ceramic filament system, for basic research efforts. The development of the two fabrication techniques to yield sheet, rod, and plate configurations with consistent and reliable properties should be undertaken for the provision of high strength-to-weight (in excess of 1.2 million inches) and high modulus-to-density (425 million inches) materials for non-corrosive environment applications.

f. Finally, the variability in composite specimens is a severe problem in the accomplishment of systematic work with pertinent variables. As such it is a severe deterrent to the generation of strong conclusions concerning the characteristics of composite materials. Concentration should be placed on the utilization of fabrication techniques which yield reliably similar composite specimens and in the improvement of reliability in the "best" fabrication techniques in the early stages of any basic or developmental program.

3. Whisker Composites
   a. The alignment of whiskers and their subsequent infiltration has been shown to yield high strength whisker composites and permits the accomplishment of high volume percent loading in addition.
   b. The nickel electrolytic infiltration technique is a model demonstration of the infiltration of an aligned whisker yarn by either electrolytic or vapor deposition molecular forming techniques.
   c. The accomplishment of higher volume percent loaded composites is envisioned as being best accomplished by the skeletal coating of whiskers in an aligned whisker yarn followed by hot pressure bonding to form a gross composite shape.
   d. The route to gross whisker composite material defined by this work involves the quantity production of spinnable whiskers, the mechanization of the whisker spinning operation based on textile technology to yield a continuous yarn, the continuous infiltration of the generated yarn by electrodeposition or vapor deposition, and the consolidation of infiltrated whisker yarns by hot pressure bonding. Such a procedure can be visualized as a production process and the product would be equivalent to current continuous fibers in its susceptibility to incorporation techniques. Uniaxial or crossply panels could be fabricated by suitable positioning of infiltrated yarns and surfaces of revolution such as pressure vessels could be wound as shapes of revolution and consolidated in a high temperature autoclave.
   e. The production development necessary to provide large quantities of spinnable whiskers has been initiated at the Thermokinetic Fibers, Inc, a subsidary of GTC. Figures 64 and 65 show complete pallets of SiC whiskers and the texture of the mats. The first step toward the mechanization of the spinning process was taken within this program and effort continues under Air Force Contract AF 33(615)-3887 which is concerned with resin and glass infiltrated aligned whisker yarns. Sapphire whiskers have been grown in spinnable form, Figure 66, to increase the number of temperature stable metal-whisker combinations. The infiltration of aligned whisker yarns by electrodeposition and vapor deposition should be concurrently developed to provide multi-matrix infiltration techniques for metals from aluminum to tungsten in temperature capabilities with the specific objective of providing a series of production techniques for infiltrated aligned whisker precursors for bulk composite fabrication.

GTC 56-44

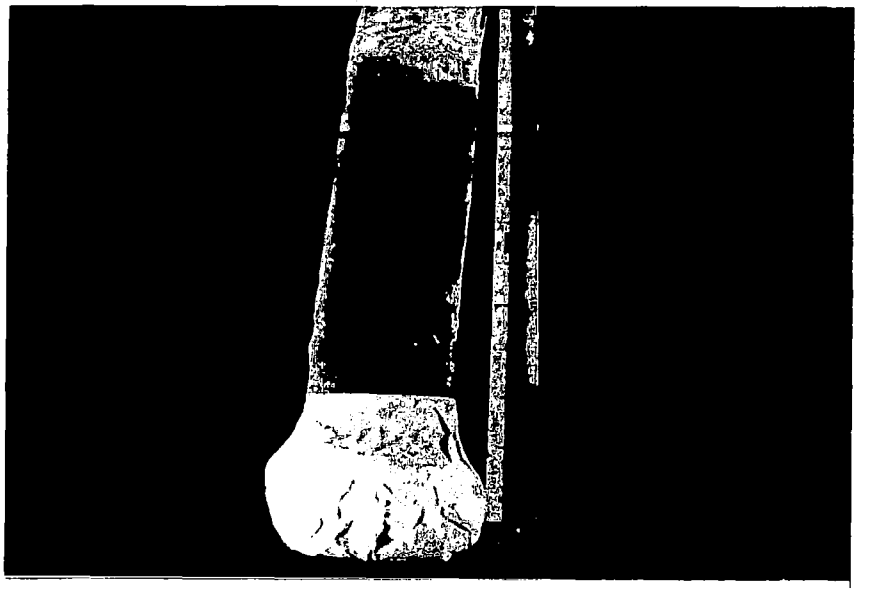

Figure 64. As Grown Pallet of SiC Whisker Wool

GTC 56-45

Figure 65. Texture of as Grown SiC Whisker Wool

GTC 56-46

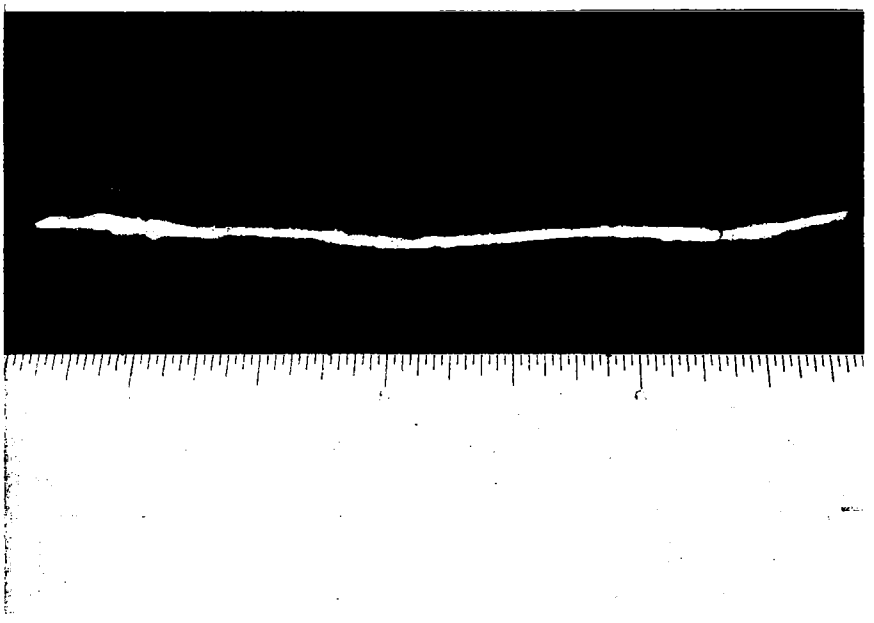

Figure 66. Dry Spun Al_2O_3 Whisker Wool Yarn

f. The properties of bulk composites formed from skeletal metal infiltrated aligned whisker yarns should be determined with the products of the infiltration program described above.

The objectives of the survey of three forms of composite materials have resulted in a series of observations, conclusions and recommendations which may be summarized as having focused the attention of potential composite researchers on the most promising presently identified avenues for further work based not on theoretical predictions but on experimental results.

REFERENCES

1. Brenner, S. S., "Tensile Strength of Whiskers", Journal of Applied Physics, December 1956, pp. 1484-1491.

2. Pearson, G. L., W. T. Read, Jr., and W. L. Feldmann, "Deformation and Fracture of Small Silicon Crystals," Acta Metallurgica, April 1957, pp. 181-191.

3. Coleman, R. V., and N. Cabrera, "Zinc and Cadmium Whiskers," Journal of Applied Physics, November 1957, p. 1360.

4. Webb, W. W., and W. D. Forgeng, "Growth and Defect Structure of Sapphire Microcrystals," Journal of Applied Physics, December 1957, pp. 1449-1454.

5. Sears, G. W., and S. S. Brenner, "Metal Whiskers," Metal Progress, November 1956, pp. 85-89.

6. Sutton, W. H. and Chorne, J., "Potential of Oxide - Fiber Reinforced Metals", Fiber Composite Materials ASM (1965), p. 173.

7. Scala, E., "Design and Performance of Fibers and Composites", Fiber Composite Materials ASM (1965), p. 131.

8. Brenner, S. S., "Factors Influencing the Strength of Whiskers", Fiber Composite Materials ASM (1965), p. 11.

9. Kelly, A. and Davies, G. J., "The Principles of the Fiber Reinforcement of Metals", Metallurgical Reviews 10, No. 37, 1965, p. 1.

10. Cratchley, D., "Experimental Aspects of Fibre-Reinforced Metals", Metallurgical Reviews 10, No. 37, (1965), p. 79.

11. Kelly, A., "Fiber-Reinforced Metals", Scientific American, February 1965, p. 28.

12. Hoffman, G. A., "The Exploitation of the Strength of Whiskers", Rand Corporation March 1958, AD 608750.

13. Hoffman, G. A., "A Survey of Development in Whisker Composites in the U. S." Rand Corporation, April 1965, AD 614991.

14. Machlin, E. S., "Status Report on Non-Metallic Fibrous Reinforced Metal Composites", M.R.C., September 1961, AD 265943.

15. Brenner, S.S., J. Metals "The Case for Whisker Reinforced Metals", 14, 1962, p. 811.

16. Sutton, W.H. and Chorne, J. "Development of High Strength Heat Resistant Alloys by Whisker Reinforcement", Metals Engineering Quarterly 3, (1963) p.44.

17. Accountices, O. E., "Whiskered Metals Reach for 1,000,000 psi", Machine Design 35, 1963 p.195.

18. "The Promise of Composites", Miler, Design Eng. Space Report 2 10 58, 1963, p.80.

19. Barkey, R.H. "Fiber Reinforcement of Metallic and Non-Metallic Composites" Clevite Corporation, Interim Report 7-924, Contract AF 33(657)-7139 February 1962.

20. Sutton, W.H., Chorne, J. Talento A, Gatti, A. Frenjold E, Brenner, S.S. and Regester R.F., Reports on Contract NOw 60-0465d, 1st, 4th, 6th, 8th, 9th, 10th, 11th, 12th, 13th, 14th, 15th, 16th, and 17th July 1960 thru September 1964.

21. Sutton, W. H., "Investigation of Bonding in Oxide-Fiber (Whisker) Reinforced Metals" General Electric Company Final Report N. AMRA Cr 63-01/8 June 1964.

22. Sutton, W.H., "Development of Composite Structural Materials for Space Vehicle Applications" Journal American Rocket Society 32 (1962), p. 593.

23. Parratt, N. J., "Reinforcing Effects of Silicon Nitride Whiskers in Silver and Resin Matrices" Powder Met 7, (1964) p. 152.

24. Kelsey, R.H., "Reinforcement of Nickel Chromium Alloys with Sapphire Whiskers" Horizons, Inc., Final Report, Contract NOw 63-0138 c, Oct 1963.

25. Parratt, N.J., "Whisker Reinforced Plastics and Metals", Chemical Engineering Progress 62, March 1966, p. 61.

26. Milewski, J.V., Shaver R.G., and Morgan, S.H., "How Whiskers Differ from Fiberglass and Boron in Characteristics and Processing Techniques", Society of Plastics Engs. Montreal, March 1966.

27. Parratt, N. J., "Reinforcement of Plastics and Metals by Silicon Nitride Whiskers" Preprint 18D Symposium on Whisker Technology AICE 58th Annual Meeting Philadelphia, December 1965.

28. Wohrer, L. C., Frechette, F and Economy, J., American Chemical Society Meeting New York, September 1965.

29. Shyne, J. J., and Shaver, R. G., "Whisker Composite Technology" Advanced Fibrous Reinforced Composites, SAMPE (1966) p. B-61

30. Wohrer, L. C. and Ecomony, J., "Single Crystal Fiber Reinforcements" Advanced Fibrous Reinforced Composites SAMPE (1966) P B-69.

31. "Whisker Technology", Chemical Engineering Progress 62 March 1966, p-3.

32. Krock, R. H., "Whisker-Strengthened Materials" International Science and Technology 59. November 1966, p. 38.

33. Shaver, Dr. R. G., General Technologies Corporation, private communication.

34. Kane, J. L. and Lindsay, E. M., "Oriented Non-continuous Fiber Reinforcement for Structural Composites", AFML-TR-65-264, August 1965.

35. Rosen, B. W., "Mechanics of Composite Strengthening", Fiber Composite Materials ASM, 1965 p. 37.

36. Alexander, J. A., Shaver, R. G., and Withers, J. C., "A Study of Low Density, High Strength, High Modulus Filaments and Composites", NASA, CR-523, July 1966.

37. Bonnano, F. R., and Withers, J. C., "The Fabrication and Mechanical Properties of SiC Filament -Metal Matrix Composites", Advanced Fibrous Reinforced Composites, SAMPE, 1966, p-F-105.

38. DeLai, A. J., Jahn, P.E., Stuhrke, W. F., and Wolff, E. G., "Fabrication of Boron Filament-Metal Matrix Composites", American Ceramic Society Meeting, May 7-12, 1966.

39. Schuerch, H., "Compressive Strength of Boron-Metal Composites", NASA CR-202, April 1965.

40. Krieder, K. G., and Leverant, G. R., "Boron Fiber Metal Matrix Composites by Plasma Spraying" AFML TR 66-219, July 1966.

41. Sinizer, D., Final Report Contract AF 33(615)-3210, October 1966.

42. Shanley, F. R. and Knapp, W. J., "Laminated Metal Ceramics Composite Materials", Sixth Sagamore Army Research Conference, 1959.